Undergraduate Dissertation

CONTEXT-AWARE PHYSICAL EXERCISE SAFETY RECOMMENDATION SYSTEM

Guilherme Shimabuko Silva Rocha

Brasilia, June 2017

UNIVERSITY OF BRASILIA

TECHNOLOGY COLLEGE

UNIVERSITY OF BRASILIA
Technology College

Undergraduate Dissertation

CONTEXT-AWARE PHYSICAL EXERCISE SAFETY RECOMMENDATION SYSTEM

Guilherme Shimabuko Silva Rocha

Report submitted to the Electrical Engineering
Department in partial fulfillment of the
requirements to obtain the degree of Electrical Engineer

Examining Committee

Antônio Padilha Lanari Bo, ENE/UnB   ————————————————
Advisor

Flávia Maria Guerra, ENE/UnB   ————————————————
Examiner

Daniel Chaves Café, ENE/UnB   ————————————————
Examiner

FICHA CATALOGRÁFICA

SILVA ROCHA, GUILHERME SHIMABUKO

CONTEXT-AWARE PHYSICAL EXERCISE SAFETY RECOMMENDATION SYSTEM / Guilherme Shimabuko Silva Rocha; Orientador: Antônio Padilha Lanari Bo; Coorientador: Ana Régia de Mendonça Neves; Coorientador: José Edil Guimarães de Medeiros. – [Distrito Federal] 2017.

x11, 61p.,210 x 297 mm (ENE/FT/UnB, Engenheiro Eletricista, Engenharia Elétrica, 2017).

Trabalho de Conclusão de Curso – Universidade de Brasília, Faculdade de Tecnologia.

Departamento de Engenharia Elétrica

1. Context Awareness	2. Bioimpedance
3. Photoplethysmography	4. Exercise Safety
5. Exercise Physiology	
I. ENE/FT/UnB	II. Título (série)

REFERÊNCIA BIBLIOGRÁFICA

SILVA ROCHA, GUILHERME SHIMABUKO (2017). CONTEXT-AWARE PHYSICAL EXERCISE SAFETY RECOMMENDATION SYSTEM, Trabalho de Conclusão de Curso em Engenharia Elétrica,Publicação 2019, Departamento de Engenharia Elétrica, Universidade de Brasília, Brasília, DF, 57p.

CESSÃO DE DIREITOS

AUTORES: Guilherme Shimabuko Silva Rocha

TÍTULO: CONTEXT-AWARE PHYSICAL EXERCISE SAFETY RECOMMENDATION SYSTEM

GRAU: Engenheiro Eletricista   ANO: 2017

_____

Guilherme Shimabuko Silva Rocha

Departamento de Eng. Elétrica

Universidade de Brasília

Campus Darcy Ribeiro

Acknowledgments

Firstly, I would like to thank all the lecturers that guided me in this project and throughout my degree. To Professor Suzete Veturelli for believing in my ability to deliver this project. To Professor José Edil de Medeiros Guimarães for accepting me at LDCI and for all of the mentoring he provided during my degree. To Professor José Camargo da Costa for allowing me to use all of the resources of his research facilities, as well as for the many teachings and mentoring. To Dr. Ana Régia de Mendonçaa Neves, for believing in this project and in my potential and for all of the advice and friendship. To Professor Antônio Padilha Lanari Bo for accepting the challenge of being my advisor and guiding me in this project's closure. To Dr. David Muir, for allowing me to develop part of this project during my exchange programme at the University of Glasgow.

Secondly, I would like to thank all of my laboratory co-workers who contributed in some way to the development of this project. I, then, extend my gratitude to the Computer Science Student Marcelo Reis, to the Electrical Engineer Reinaldo Gutierrez Pimenta, to the Computer Engineers Matheus Souto Bastos and Tiago de Melo Tiveron Borges and to the Biomedical Engineering Student Carlos Meneghini for all the dedications, sacrifice and fellowship.

I would also like to thank my co-workers at DFchip, LDCI, LARA and Midialab who accompanied me in this journey and who at some moments pointed me to the right path. From those, I would like to emphasize my gratitude to my boss and friend, Dr. Heider Marconi, for all of the mentorship who helped shaping me as a professional.

No less important in this journey were the many friends who gave me psychological and emotional support everytime I needed and whose names are too many to list. A special thanks to Pedro Henrique Françaa, childhood friend, Natasha Huang, Marcos Guo Yan and Daniel Akira Ando for making the path less challenging, Camilla Oliveira, Elena Pinheiro, Vinícius Santos, Rayanne Rodrigues, Giovanna Teixeira and Rafaela Parisotto for being by my side in times of need.

Lastly but not least, I would like to thank every member of my family that somehow contributed to shape the person I am today and who gave me the necessary support to be here today.

Guilherme Shimabuko Silva Rocha

ABSTRACT

Although recent researches corroborate with previous findings regarding the benefits of practising regular physical activities, doing so in unfavourable conditions can also be harmful to an individual's health. In this sense, this dissertation brings an electronic and computational approach to helping people in the safe practise of exercise by using contextual information such as resting heart-rate, Body Mass Index (BMI), Body Composition, environmental temperature and air humidity to provide the user with contextualised recommendation.

In order to achieve this, a recommendation system was developed to acquire the necessary data, process it and provide useful guidance. A preliminary version of the system was developed as a proof-of-concept implementation that would receive most of the data as a user provided input and generate the recommendation. Later, each data acquisition module of the system was individually designed and validated by means of simulations, testbenches or even comparison with similar available devices when relevant. These tests proved that, although there is room for improvement, that each circuit designed was able to successfully measure the variables in question. The pulse rate monitor was compared to different commercial devices and presented similar readings and the Bioimpedance Analysis Device accurately measured the impedance from the circuits modelling a human body. This project was developed as a partnership between MidiaLab, LDCI and LARA at the University of Brasilia. Part of this project was also developed during an exchange programme at the University of Glasgow

RESUMO

Embora pesquisas recentes corroborem com resultados prévios a respeito dos benefícios da prática regular de atividades físicas, realizá-las em condições desfavoráveis pode ser prejudicial à saúde do indivíduo. Neste sentido, este trabalho apresenta uma abordagem eletrônica e computacional que visa ajudar as pessoas na prática segura de exercícios físicos utilizando informações a respeito do contexto como: a frequência cardíaca de repouso, o índice de Massa Corporal (IMC), a composição corporal e a temperatura e a umidade do ambiente, para fornecer ao usuário uma recomendação contextualizada.

Buscando alcançar esse objetivo, um sistema de recomendação foi desenvolvido para adquirir os dados necessários, processá-los e prover uma sugestão proveitosa. Uma versão preliminar do sistema foi desenvolvido como uma implementação da prova de conceito que receberia a maioria dos dados como uma entrada fornecida pelo usuário e geraria uma recomendação. Posteriormente, cada módulo de aquisição de dados foi individualmente projetado e validado por meio de simulações, testes de bancada, ou até mesmo por comparação com dispositivos similares disponíveis quando fosse relevante. Esses testes provaram que, embora haja possibilidade de melhorias, os circuitos projetados foram capazes de realizar as medições necessárias com sucesso. O monitor de pulsos foi comparado com diferentes dispositivos comerciais e apresentou leituras similares e o dispositivo de analise de bioimpedância mediu com acurácia as impedâncias dos circuitos usados para modelar um

coropo humano. Este projeto foi desenvolvido como uma parceria entre os laboratórios MidiaLab, LDCI (Laboratório de Dispostivos e Circuitos Integrados) e LARA (Laboratório de Robótica e Automação) na Universidade de Brasília. Parte dele também foi desenvolvida durante intercâmbio na Universidade de Glasgow.

TABLE OF CONTENTS

FIGURES LIST

TABLES LIST

Chapter 1

Introduction

1.1 Contextualisation

Two of the major risks factors for heart diseases and other chronic diseases such as diabetes and cancer are overweight and obesity, which are estimated to be responsible for at least 2.8 million deaths every year worldwide, according to the World Health Organization (**WHO**) in [1]. In a world where obesity rates have nearly doubled since 1980 (**WHO** in [2]), finding out how to control this issue's growth is a pressing matter.

WHO also states that one of the ways of reducing obesity on a societal level is to support individuals in engaging in regular physical activity. Besides, the same organisation affirms in [3], that during the year of 2008, 31% of adults worldwide aged 15 or more were considered to be insufficiently active. Estimates say that insufficient physical activity may cause the deaths of 3.2 million people every year around the globe (**WHO** in [3]).

The inadequate practice of physical activities may be just as harmful as the lack of it. As Marins states in [4], the practice of physical exercises at unfavourable conditions, such as high temperature and humidity, may provoke thermal stress to an individual, which ultimately can even lead to death. Considering these circumstances, a system capable of warning the user about the safety of practising physical activities becomes relevant.

1.2 Problem Definition

With the development and popularisation of mobile technology and wireless networks, a new paradigm, called context-aware computing [5], arises with the purpose of improving the user-environment interaction. In such a scenery, applications start to consider the user's current situation to provide relevant and accurate information and services. In this context, project BioCyberUrban ParQ [6] was developed aiming at improving the interaction between the user and the Sarah Kubitschek Park (Brasilia's City Park) by means of pervasive and ubiquitous computing systems. The system proposed in this dissertation, called Smart Bench, is part of this project and

intends to provide physical exercises practitioners with contextualised recommendation according to the user's biomedical data and information about the weather. It consists of a modified bench fitted with several sensors, and the necessary signal conditioning circuitry that communicates with a totem via an Arduino. The totem will then process the data and turn it into a recommendation and display it to the user through a friendly graphical interface.

It is important to highlight that the system described in this dissertation is not intended as a replacement for professional consultation or clinical usage. It is merely a tool that provides everyday suggestions regarding the safe practice of physical activities based on scientific analysis on data that otherwise would be scattered.

1.3 Project Goals

The main goal of this work is to design and implement circuits capable of obtaining relevant biomedical and weather-related data as well as develop an application capable of using this context to provide useful recommendations regarding the safe practice of physical activities. The list below describes the specific objectives that must be completed to achieve this goal.

- Design and implement a module capable of adequately measuring local temperature and air humidity;

- Design and implement a module capable of acquiring the user's resting pulse-rate;

- Design and implement a module capable of measuring the user's body Mass;

- Design and implement a user-system interface to allow input of the required information to compute the user's BMI and Body composition;

- Design and implement a module capable of estimating the user's body composition;

- Test and Validate the modules developed in the items above;

- Integrate all modules into a single data processing unit;

- Develop an application capable of using the data obtained by the aforementioned data to create a context-based recommendation;

1.4 Manuscript Presentation

Chapter 2 provides a literature review of the various concepts used in this project's implementation. Chapter 3 describes the methodology used to develop the project. The experiments performed to validate the system are discussed in Chapter 4, immediately followed by conclusions and a discussion of possible ideas related to the project that were not yet implemented in Chapter 5. Annex I is aimed at readers from fields related to Biomedical Engineering and Exercise Physiology who do not posses extensive knowledge on the core concepts of Electrical and Electronics

Engineering in an attempt to level the understanding of this manuscript. It contains a brief explanation on the functioning of basic filters and amplifiers which is required to understand the designs described in this manuscript.

Chapter 2

Literature Review

2.1 Introduction

Due to the multidisciplinary nature of this system, the following sections will review the theory in the field of Exercise Physiology which will justify why each variable is important to the generation of a recommendation. Following this, oscillator topologies and their analysis will be presented as this knowledge is of paramount importance to the full understanding of this manuscript.

2.2 Weather Conditions

2.2.1 Impact of Weather on Physical Activities Safety

According to Seeley[7], it is considered that the average normal temperature of the human body is 37°C (98.6°F), if measured orally, and 37.6°C when measured rectally. Since heat is naturally generated by the normal metabolism, to ensure constancy of the body temperature, which is essential to maintain homeostasis, heat has to be exchanged with the environment. This can be achieved by radiation, conduction, convection, or even evaporation of water in the body surface.

Mechanisms such as perspiration of the skin or muscle contractions of shivering are natural ways of controlling these heat exchanges to ensure that the body remains in the desired temperature. When for some reason these mechanisms are not enough to maintain the normal temperature, two situations may arise. (i)Hyperthermia, i.e when the body's capacity to lose heat is exceeded by the gain and production of heat by the body, or (ii)Hypothermia, when the loss of heat is greater than the body's ability to produce it.

In hot and humid environments, the evaporation of sweat is compromised due to the excessive humidity. In addition to that, if the environmental temperature is higher than the body, there will be gain of heat from the environment and the loss of heat through convection is impaired. As a result of that, to prevent overheating, it is advisable to limit the practice of physical exercise in such a scenario.

Table 2.1, adapted from [8], correlates air temperature and relative humidity to heat sensation and highlights some of the possible negative outcomes of exercising in unfavourable weather conditions due to thermal stress. For instance, exercising under a heat sensation between 90°F and 105°F may lead to cramps, while between 105°F and 130°F, not only cramps are more likely, but there is also the possibility of heat strokes. Practising such activities at temperatures above 130°F will subject a person to a very high risk of heat strokes, possibly even leading to death. These guidelines were used in the system to quantify the safety of practising physical activities for the measured weather conditions.

Table 2.1: Table describing possible negative outcomes of exercising in unfavourable weather conditions.

	Air Temperature (°F)										
	70	75	80	85	90	95	100	105	110	115	120
Relative Humidity	Heat Sensation (°F)										
0,00%	64	69	73	78	83	87	91	95	99	103	107
10,00%	65	70	75	80	85	90	95	100	105	111	116
20,00%	66	72	77	82	87	93	99	105	112	120	130
30,00%	67	73	78	84	90	96	104	113	123	135	148
40,00%	68	74	79	86	93	101	110	123	137	151	
50,00%	69	75	81	88	96	107	120	135	150		
60,00%	70	76	82	90	100	114	132	149			
70,00%	70	77	85	93	106	124	144				
80,00%	71	78	86	97	113	136					
90,00%	71	79	88	102	122						
100,00%	72	80	91	108							

90-105°F	Possibility of Heat Cramps
105-130°F	Heat Cramps or Heat Exhaustion Likely, Heat Stroke Possible
>130°F	Heat Stroke a Definite Risk

2.2.2 Measuring Temperature and Humidity

The American National Research Council defines in [9] sensor elements as a fundamental transduction mechanism that converts one form of energy into another and sensors as one or more sensor element with a physical packaging and external connections. The same text claims that records of temperature sensors that use the temperature sensitivity of electrical resistance in different materials can be tracked to even to the early 1860s, when Wilhelm Von Siemens developed a copper based temperature sensor.

Farahani et al. describe in [10] as the amount of water vapour in an atmosphere of air or other gases and explains that some sensors, categorised as hygrometric sensors, use the changes in electrical conductance or capacitance of certain materials due to the absorption or desorption of water molecules from the air. Hygrometric sensors can also be classified into ionic or electronic

conduction sensors depending on the type of carriers used to perform electrical transportation.

A compound sensor can be designed by using sensor elements capable of measuring both physical quantities to properly assess weather conditions.

2.3 Pulse Rate Monitor and Resting Heart Rate

2.3.1 Resting Heart Rate and Fitness Levels

As Seeley affirms in [7], exercise training increases athletic performance due to the cardiovascular and respiratory systems becoming more efficient. Table 2.2, adapted from the Aquatic Exercise Association in [11], shows how the resting heart rate can be used to assess an athlete's fitness levels. It establishes a relationship between gender, age, heart rate and physical condition. Generally speaking, lower heart rates tend to indicate higher pulmonary capacity, and therefore, higher fitness levels. Since, the metabolic needs of a human change with age and gender, so does the need for oxygen, which is why the exact ranges of resting heart rate that define a certain fitness level vary with those two other variables. For instance, For a male between 18 and 25 years old, a resting heart rate of 49 to 55 bpm will indicate an excelent fitness level, for a female older than 65 years old is classified with the same fitness level with 54 to 59 bpm.

Table 2.2: Table showing the relationship between fitness levels and Resting Heart Rate (beats/min).

Age (Years)	18-25		26-35		36-45		46-55		56-65		>65	
Gender	M	F	M	F	M	F	M	F	M	F	M	F
Excelent	49-55	54-60	49-54	54-59	50-58	54-59	50-57	54-60	51-56	54-59	50-55	54-59
Good	56-61	61-65	55-61	60-64	59-62	60-64	58-63	61-65	57-61	60-64	56-61	60-64
Above Average	62-65	66-69	62-65	65-68	63-66	65-69	64-67	66-69	62-67	65-69	62-65	65-68
Average	66-69	70-73	66-70	69-71	67-70	70-72	68-71	70-73	68-71	70-73	66-69	69-72
Below Average	70-73	74-78	71-74	72-76	71-76	73-78	72-76	74-77	72-75	74-77	70-73	73-76
Poor	74-81	79-84	75-81	77-82	77-82	79-82	77-82	78-84	76-81	78-81	74-81	77-79
Very Poor	>=82	>=84	>=82	>=83	>=83	>=83	>=83	>=83	>=82	>=82	>=82	>=80

Hong Kong's Department of health's guidelines in [12] affirms that sedentary individuals would be the ones to accrue the most benefits in fitness outcomes from increasing the practice of physical activities. In their handbook, it is recommended that for such individuals, moderate intensity aerobic exercises should be prescribed. It is also advised that sedentary people should build up their physical activity targets over several weeks to minimise muscle soreness and fatigue.

The Smart Bench system uses the information of the table to classify the likelihood of a certain user to be sedentary, or active based on their fitness levels and then assess the risk of fatigue and muscle soreness, as well as the benefits of certain activities over others.

2.3.2 Photoplethysmography

To assess the user's resting heart rate, a simple pulse rate monitor was built using a technique known as Photoplethysmography. According to Allen in [13] "Photoplethysmography (**PPG**) is a simple and low-cost optical technique that can be used to detect blood volume changes in the microvascular bed of tissue". This technique can be used to build pulse rate monitors. The technique consists in focusing a beam of red or near-infrared light on the target tissue and measuring either the resultant reflection or the transmittance of light through the tissue. Due to the light's limited power of penetration, this measurement is usually done in fingertips, or earlobes. This technique was used to build a simple Pulse-rate monitor aiming at assessing the user's resting heart-rate. Other data that can be obtained using photoplethysmography include but is not limited to oxygen saturation, blood pressure cardiac output (Allen in [13]).

In the history of Photoplethysmography, some factors were found to be of great influence to the final result. For instance, when it comes to light-tissue interactions, the choice of the light source is of utmost importance. This happens because, when choosing the light source for a **PPG** based device, the first concern is if the light will be able to penetrate the tissue. For that, it cannot be highly absorbed by water, the main component of human body, nor by the melanin. This fact alone already narrows the spectrum of light to red and near infrared light. This window in the water's absorption spectra is called *The Optical Water Window* [13]. Secondly, for the specific application covered by this manuscript, ideally the light absorption should not be influenced by oxygen saturation, as this changes in time independently of the heart rate. Since there is a sensitive difference between the absorption of light between Oxyhaemoglobin (HbO2) and Haemoglobin(Hb) except at the *Isobestic Wavelength*, i.e close to $805\eta m$, the light source should be selected to be as close to this value as possible[13]. With that in mind, the Smart Bench system was designed with a TCRT1010 reflective optical sensor which emits light at a $950\eta m$.

2.4 Body Mass Index (BMI) and Body Composition

To further assess the subject's physical fitness, it is also important to evaluate the Body Mass Index, and the body composition. This is done to ensure that the user will receive a recommendation that is compatible with his or her current physical capabilities and needs. The body mass index is, according to The Scottish Intercollegiate Guidelines Network (**SIGN**) in [14] "[...] a measure of weight status at an individual level and takes account of the expected weights in adults of different heights."The equation to calculate BMI, also from SIGN in [14] is defined by equation 2.1 where the weight is given in kilograms and the height in meters.

$$BMI = \frac{Weight}{height^2} \tag{2.1}$$

In order to predict the body composition from the bioimpedance, the equations 2.2 and 2.3 presented by Wan, et al. in [15] can be used.

$$FFM = 0.661\frac{H^2}{R_{50}} + 0.2W - 0.32 \qquad (2.2)$$

$$TBW = 0.4\frac{H^2}{R_{50}} + 0.148W + 3.32 \qquad (2.3)$$

Where FFM stands for Fat Free Mass, TBW for Total Body Water, H is height in centimeters, W is Weight in kilograms, and R_{50} is the subject's body resistance measured with a $50kHz$ current.

This data is obtained through three different modules: a weight scale, a device developed for this system that is capable of estimating the user's bioimpedance, and a user interface to obtain the necessary data from the individual. The combination of these measurements, as well as the resting heart rate, allows the separation of individuals with high **BMI**, but low body fat percentages, low **BMI** but high body fat percentages and even between active obese people and sedentary obese people, which grants a better assessment of their real fitness levels.

The Scottish Intercollegiate Guidelines Network (**SIGN**) defines in [14] a classification of healthy weight ranges according to a subject's **BMI**. This classification can be seen in Table 2.3.

Table 2.3: Fitness levels according to healthy **BMI** ranges (Scottish Intercollegiate Guidelines Network).

Classification	Underweight	Healthy	Overweight	Obesity 1	Obesity 2	Obesity 3
BMI(kg/m^2)	$<= 18.5$	18 to 24.9	25 to 29.9	30 to 34.9	35 to 39.9	$>= 40$

Also, the American Council on Exercise details in [16] a relationship between fitness levels the body composition of the subject, more specifically the body fat percentage. This relationship is described in Table 2.4.

Table 2.4: Fitness levels according to body fat percentage ranges (American Council on Exercise).

	Essential	Athletes	Fitness	Average	Obese
Male	2% to 5%	6% to 13%	14% to 17%	18% to 24%	>25%
Female	10% to 13%	14% to 20%	21% to 24%	25% to 31%	>32%

2.4.1 Exercise Recommendation Guidelines based on Fitness levels

As a general recommendation to treat obesity, the Scotish Intercollegiate of Guidelines Network claims in [14] that adults should be prescribed a volume of physical activity equivalent to the expenditure of approximately 1800 to 2500 kcal per week (roughly corresponding to 225 to 300 minutes of moderate activity per week). While it suggests that individuals should be encouraged to engage in physical activities, the same document states that obesity increases the risk of diabetes, cancer, heart and liver diseases, ashtma, osteoarthritis and other comorbidities and as such, the prescription of exercises may warrant some adaptations. As McQueen says in [17], "Obese exercisers may require accommodations for arthritic conditions, and modifications of weight-bearing activities may

be necessary. [...]Obese individuals are also at increased risk for hyperthermia, and the exercise environment should be appropriately adapted.". Hong Kong's Centre for Health Protection advises in [12] that for overweight and obese people, brisk walking constitutes moderate intensity activity and warns that people with **BMI** over $35kg/m^2$ may present difficulty even with weight bearing activities. For these individuals, it is recommended to gradually increase the practice of moderate activities such as cycling, swimming and other forms of aerobics.

2.4.2   Bioimpedance Analysis

Bioimpedance Analysis is a simple, quick, noninvasive method that is widely used to estimate body composition as defined by Wan et al. in [15]. The electrical impedance of a circuit element, as Lipiansky describes in [18], is the ratio of the voltage phasor (measured in the terminals of the element) to the current phasor passing trough the element at one angular frequency for sinusoidal voltage and current waveforms. As a complex quantity, it has a real component (resistance) and an imaginary component (reactance). The former is the major opposition of the conductor to the passage of electrical current while the latter is an additional opposition created by the storage of electric charges by reactive components over time. **BIA** is defined as the measurement of the opposition that biological tissues pose to the flow of a small alternating current (usually smaller than 1 mA)(National Institute of Health, United States, in [19]). In the human body, at low enough frequencies, the resistance is mainly composed of the extra-cellular part of non-adipose tissue and the reactance is mainly derived from the lipid component of the cellular membrane, tissue interfaces and nonionic tissues which act as capacitors (Dehgan in[20]). As a result of this, the human body can be modelled as a simple capacitive circuit such as the one used in [21] and shown in Figure 2.1, in which a resistor is connected in parallel to a capacitor. The National Institute of Health of the United States (**NIH**) affirms in [19] that the typical resistance measured in human beings is around 250Ω, which usually represents 90% of the impedance value and that **BIA** devices should be able to operate adequately within a range around these values, suggesting a test impedance of 1000-j500Ωwith an accuracy of 1%. The resistance and capacitance from the model can then be calculated to be within the suggested values, so that the designed device can be simulated and tested for more realistic scenarios.
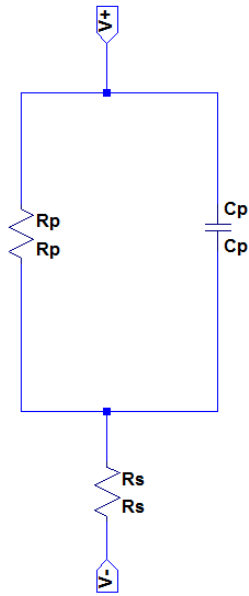
Figure 2.1: Equivalent circuit usually found in the literature.

Although this approach has been widely used, a different equivalent circuit was suggested by Chinen et al. in [22]. This circuit, shown in the Figure 2.2, was obtained from the measurement of the frequency response of the human body, when the frequency of a voltage source was varied.
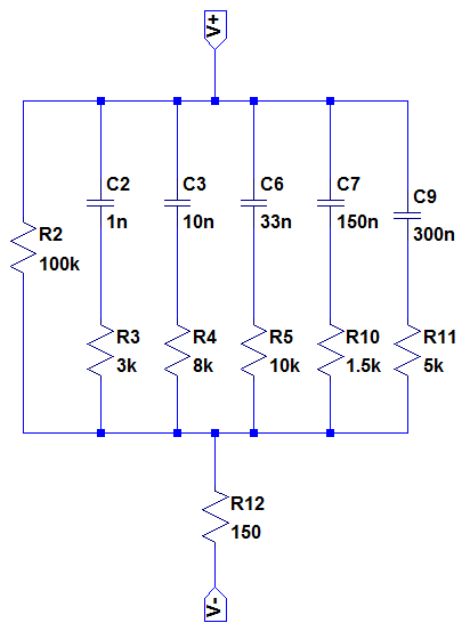
Figure 2.2: New equivalent circuit model with 5 High Pass Filters obtained from frequency response experiments.

The initial experiment with low frequencies suggested that the human body was equivalent to a combination of RC High-Pass Filters, which was confirmed by further experiments described in the same article. Table 2.5 from [22] shows the resulting resistances for the equivalent circuit

suggested for three different electrode positioning setup.

Table 2.5: Numerical values of the circuit elements for calculation of impedance for three different electrical paths of a human body obtained from a Frequency Response Analysis.

|	$R_{\_}(\Omega)$	$R_2(k\Omega)$	$R_3(k\Omega)$	$R_4(k\Omega)$	$R_5(k\Omega)$	$R_6(k\Omega)$	$R_7(k\Omega)$	$C_1(\eta F)$	$C_2(\eta F)$	$C_3(\eta F)$	$C_4(\eta F)$	$C_5(\eta F)$
Right to Left Hands	150	100	3	8	10	1.5	5	1	10	30	150	0.3
Right to Left Armpits	30	10	1.5	8	8	1	1.5	1	10	30	80	0.3
Both Armpits to Both Feet	50	10	0.5	1.5	1	1	0.3	5	10	30	80	1

To ensure more comprehensible results, both circuits were used in the simulation and in the designed testbench experiments.

2.5 Oscillators

Oscillators are, as defined by Razavi in [23], circuits that produce and indefinitely sustain periodic outputs, usually voltage, with no input. This kind of circuit is essential in many electronic systems and can be built with several different topologies depending on its use. This subsection will describe the basis for an oscillator project, and present a few possible topologies.

The first concern when designing an oscillator is to build a circuit capable of oscillating in a defined frequency. Still according to Razavi in [23], oscillations may occur in a circuit if the phase shift at high frequencies is so big that the overall feedback becomes positive, yielding a closed loop gain close to infinity at the desired frequency. The Barkhausen Criteria define two necessary but not sufficient conditions for a circuit to oscillate. The first, already mentioned, is that the total phase shift of the loop gain must be equal to $360°$ or to an integral multiple of $360°$. The second criterion states that for a circuit to oscillate, it must have a loop gain with magnitude greater or equal to one. Mathematically, the Barkhausen criteria can be described by equations 2.4 and 2.5.

$$|H(j_w0)| >= 1 \tag{2.4}$$

$$\angle H(j_w0) >= 180° \tag{2.5}$$

For a system with a transfer function given by

$$\frac{Y(s)}{X(s)} >= \frac{H(s)}{1 - H(s)} \tag{2.6}$$

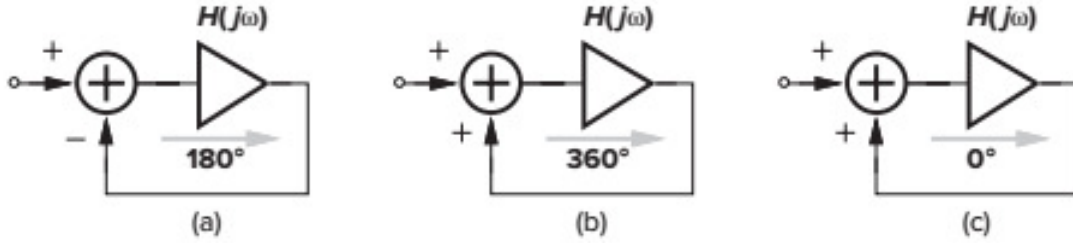Graphically, this system can be seen in Figure 2.3 adapted from Razavi [23].

Figure 2.3: Different views of an oscillatory system

2.5.1 Ring Oscillators

One of the simplest topologies for oscillators is that of the Ring Oscilators. They are made of an odd number, equal or greater than three, of connected inverters with feedback as stated by Aluru in [24] as shown in the Figure 2.4 from Razavi in [23].
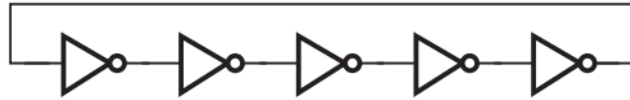
Figure 2.4: Five-Stage single-ended ring oscillator

In such an oscillator, each node of the circuit will oscillate according to the equation 2.7 shown by Aluru in [24].

$$f = \frac{1}{N(t_{PHL} + t_{PLH})} \tag{2.7}$$

Where N is the number of inverters, t_{PHL} is the propagation delay of a signal from High to Low and t_{PLH} is the progagation delay of a signal from Low to High. Although these circuits are easily built, the waveform hardly resembles a sinusoidal signal, so it may not be adequate to certain applications.

2.5.2 LC Tank Oscillator

In [23], Razavi shows that when an inductor is placed in parallel with a capacitor (Figure 2.5 adapted from Razavi in [23]), the circuit resonates at a frequency described in equation 2.8. In this frequency, the impedance in these two components will have equal magnitude, but opposite signals, yielding an infinite resulting parallel impedance.

$$f = \frac{1}{\sqrt{LC}} \tag{2.8}$$

In practice, though, both the inductors and capacitors will have a parasitic resistance, which means that the impedance will not go to infinity and the oscillations will eventually fade. To

compensate for this, LC tanks tend to be used as tuned circuits in feedback loop stages to define the oscillation frequency such as the circuit seen in Figure 2.5 adapted from [23].

(a) LC Tank Circuit

(b) Tuned gain stage in feedback loop
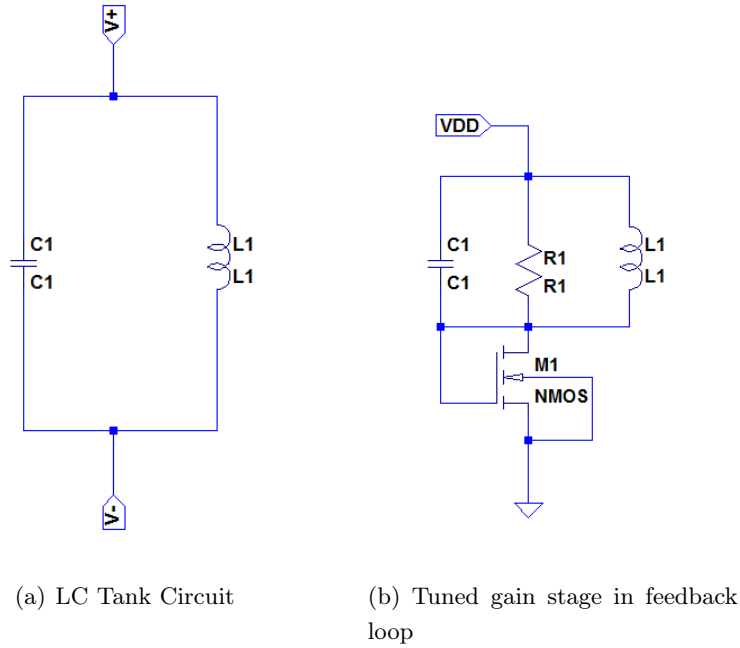
Figure 2.5: Oscillators based on LC tank.

2.5.3 The Hartley Oscillator

The Hartley Oscillator circuit is an analogous of a Collpits Oscillator that uses two inductive coils and a capacitor as its tuning circuit to define both resonant frequency and feedback magnitude as described by Rao [25]. One possible configuration for this circuit uses a BJT in a common emitter configuration as its basic amplifier. The circuit in Figure 2.6 from Rao [25] shows one of the possible ways of making a Hartley Oscillator. In this configuration, the feedback from the voltage between L1 and L2 and the common emitter operation of the transistor generate a total phase shift of 360°, satisfying one of the Barkhausen Criteria for oscillations. The second part of the criteria is satisfied when the inequation 2.9 is satisfied.

$$A_v = \frac{r_c}{r_e} > \frac{L_2}{L_1} \tag{2.9}$$

And the frequency of the tuning circuit is calculated as:

$$f_0 = \frac{1}{2\pi\sqrt{(L1 + L2)C}} \tag{2.10}$$
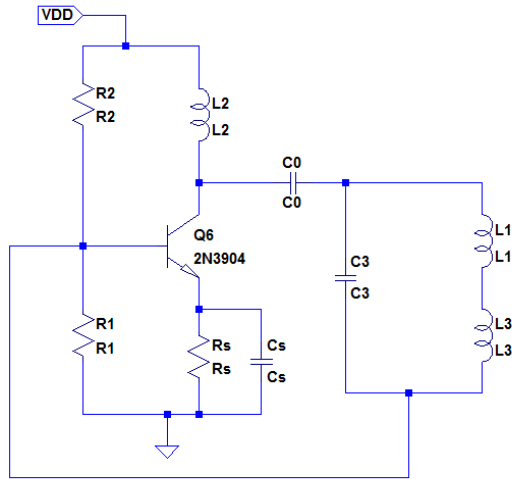
Figure 2.6: One possible form of the Hartley Oscillator topology.

2.5.4 Relaxation Oscillator

The Relaxation Oscillator, also known as the Astable Multivibrator is a circuit that employs an operational amplifier as a comparator with positive feedback to generate symmetrical square wave signals. The schematic for this circuit can be seen in Figure 2.7 adapted from Senani, et.al from [26]
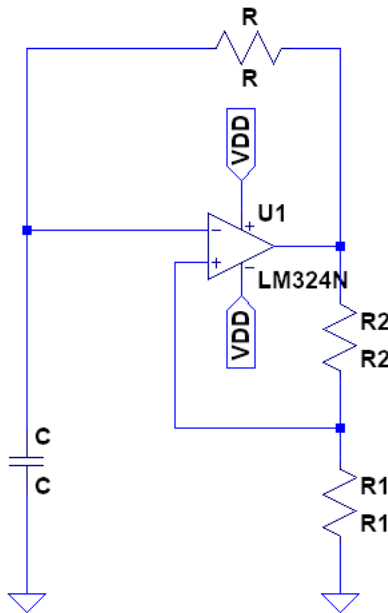
Figure 2.7: Schematic for a Relaxation Oscillator, also known as an Astable Multivibrator.

The oscillation frequency for this circuit is given by the equation 2.11, and further details on the oscillator's operation is described in Senani, et al [26].

$$f = \frac{1}{2RCln(\frac{1+\beta}{1-\beta})} \tag{2.11}$$

Where β is defined by 2.12.

$$\beta = \frac{R1}{R1 + R2} \tag{2.12}$$

Chapter 3

Development

3.1 Introduction

As explained in Section 1.2, the Smart Bench project was initially developed as a part of the ParQ project in the form of a partnership between two laboratories from the University of Brasilia: Midialab (a computational arts and technology laboratory) and LDCI (an integrated circuits and electronic devices laboratory). As time moved on, more people were invited to contribute, and a prior version of the system was presented at an Arts and Technology Conference [27] and as a graduation project for two students from the Higher Education Institute of Brasilia (IESB) [28]. Later, one of the modules was improved and tested at the University of Glasgow as part of a Science Without Borders Exchange and ultimately it was brought back to the University of Brasilia where it is being finalised by the Laboratory of Automation and Robotics (LARA).

Rather than follow a chronological sequence of events, aiming at a better understanding of the system's development, the next section will dissect its architecture and each one that follows will detail the conception of each module.

3.2 General Architecture

The architecture described in this section comprises of a Temperature and Humidity sensor (Section 3.4), a Pulse Rate Monitor (Section 3.6), and a Bioimpedance Analysis Device (Section 3.7), all connected to an Arduino controlled by a user interface (Section 3.3). The arduino is also connected through a local network to the Java Application (Section 3.8) that monitors the weight scale, generates the recommendations and controls a second user interface. These connections are illustrated in Figure 3.1.
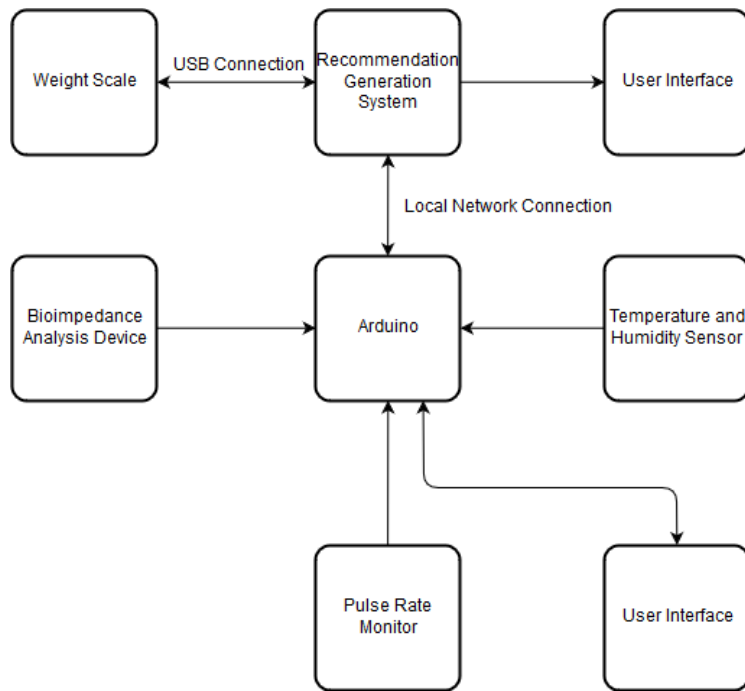
Figure 3.1: Block Diagram showing the connection between the different modules of the system.

3.3   User Interface

The user interface of the system comprises two separate parts. The first allows the user to insert information that would be impracticable to measure but paramount for the proper assessment of fitness conditions such as age, height, and gender, while the second works as a display for the measurement and computation results.

The interface built to insert data is made of an LCD display (to ask the user the required question), a knob (to allow the user to choose an answer) and two buttons (one to advance to the next question and another to return to the previous one). The schematics in Figure 3.2 shows the use of a pull-down resistor in both the forward (a) and return (b) buttons to ensure that the signal sent to the Arduino would be a Digital High when the button was pressed and a Digital Low when the button was not being pressed.

(a) Forward Button.
(b) Return Button.
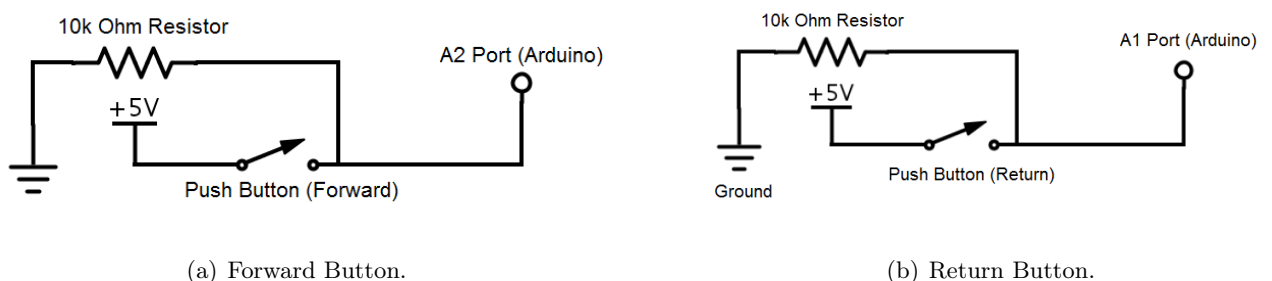
Figure 3.2: Schematics for the buttons that allowed a user to interact with the system.

Figure 3.3 shows a simple connection between a potentiometer and the Arduino to create a

selection knob.
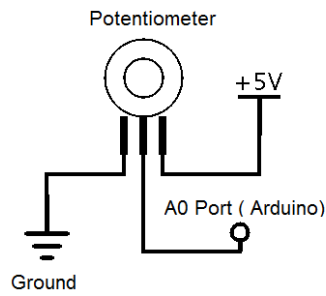
Figure 3.3: Schematic of the selection knob built using a potentiometer.

To complete the bench user interface, Figure 3.4 shows the LCD display that presents the required inquiries.
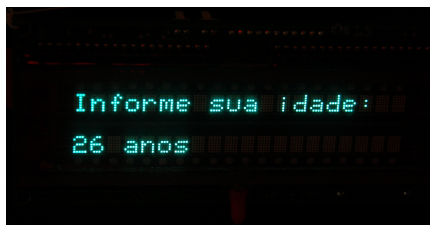
Figure 3.4: LCD Display responsible for presenting the user with necessary inquiries.

The second part of the interface is what the system will display after the data is processed. As it can be seen in Figure 3.5, if no measurement has been taken from any individual, the screen shows a frame with the temperature and humidity at that moment and a generic recommendation regarding the weather conditions and how it should affect an exercise routine.

Figure 3.5: Frame with general recommendation related solely to the weather.

In case an individual uses the bench to interact with the system, after all measurements are taken and all computations are made, the totem will show a different frame with a personalised recommendation and the data of interest to the user as shown in Figure 3.6.
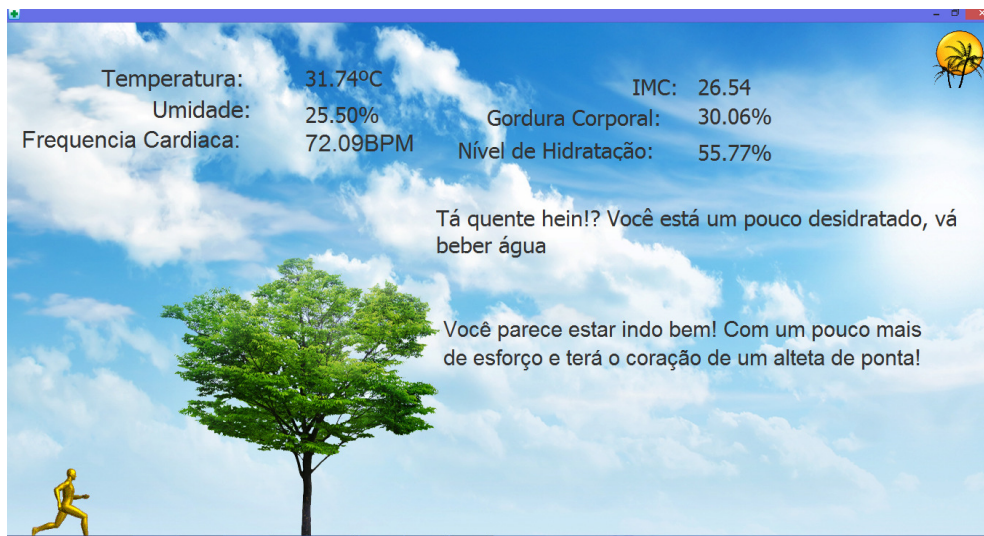
Figure 3.6: Frame for personalised recommendation based on biomedical and weather related data.

3.4 Temperature and Humidity

The acquisition of environmental variables such as temperature and humidity can be achieved by the use of sensors, in this case the Temperature and Humidity Sensor - RHT03 was used. As the manufacturer claims in [29] the RHT03 is a low power sensor suited for harsh environments and delivers an accurately calibrated, temperature compensated, digital output signal.

As explained in the arduino library DHTLib documentation [30], the RHT03 is an equivalent to the DHT22 sensor, and as such can be controlled by it.
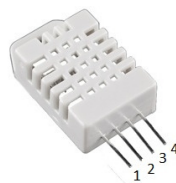
Figure 3.7: Temperature and Humidity Sensor - RHT03.

Since the output from this sensor is a calibrated digital signal, no conditioning circuits were needed and the connection scheme for the RHT03 is described in the Table 3.1

Table 3.1: Table detailing RHT03 connections.

Sensor Pins	Connections
1	5V
2	PIN D2 (Arduino)
3	Not Connected
4	GND

3.5 Weight Scale

Originally, the weight scale was a simple commercial device with built-in bioimpedance analysis capabilities, but as the project evolved the need for a custom made module arose. To fulfil all of the project's requirements, 4 Phidget's Load Cells ($CZL635 - 3134\_0$), with the capacity to measure up to 50 kg each, were used. In addition to that, an interface board for load cells and wheatstone sensors called "1046 - Phidget Bridge 4-Input" was used to amplify and process the signal from the $CZL635 - 3134\_0's$.

Since the "1046 - Phidget Bridge 4-Input" uses a USB connection and personalised libraries in several languages to communicate with a computer application, this device would easily be incorporated into the system, provided a few changes were made. The personalised Java Library, allowed direct connection to the Java application, but it also required that the weight scale and the monitor displaying the user interface had a physical cabled connection.

A simple algorithm was developed to calibrate the weight scale, in which the system would recognise if the output of the sensors was similar to the expected scale structural weight and discount this value from the measurements. Then, a test platform was built using wood and acrylic. Even though the prototype in Figure 3.8 allowed for primary tests, it was too fragile for human trials and it still has to be replaced by a sturdier version. Due to this, the weight scale did not go through further assessment and therefore it is not present on Chapter 4.
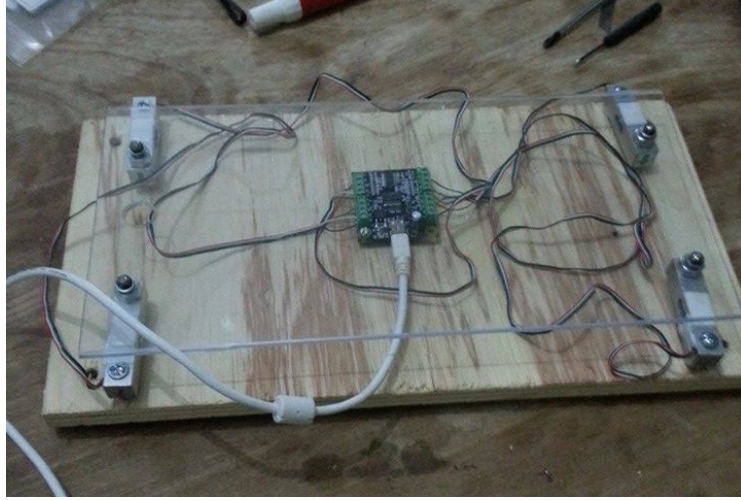
Figure 3.8: Weight scale prototype made in acrylic and wood to allow tests and calibrations to be performed on the module.

3.6 Pulse Rate Monitor

The first pulse rate monitor used on the system was an adaptation of an early implementation of the EasyPulse project published by Bhatt at [31]. This design, shown in Figure 3.9, used a high gain operational amplifier and a Bipolar Junction Transistor Amplifier to transform the signal, obtained from a transistorised infrared reflection sensor called TCRT5000, into a quantised square wave with a frequency equal to the pulse rate. Then, a simple pulse detection algorithm, described in Figure 3.10, would calculate the pulse rate.
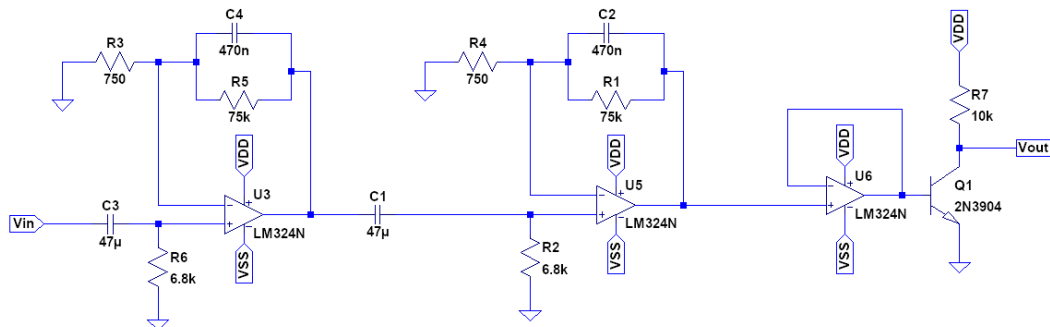
Figure 3.9: Pulse rate detection circuit based on the Easy Pulse Project.
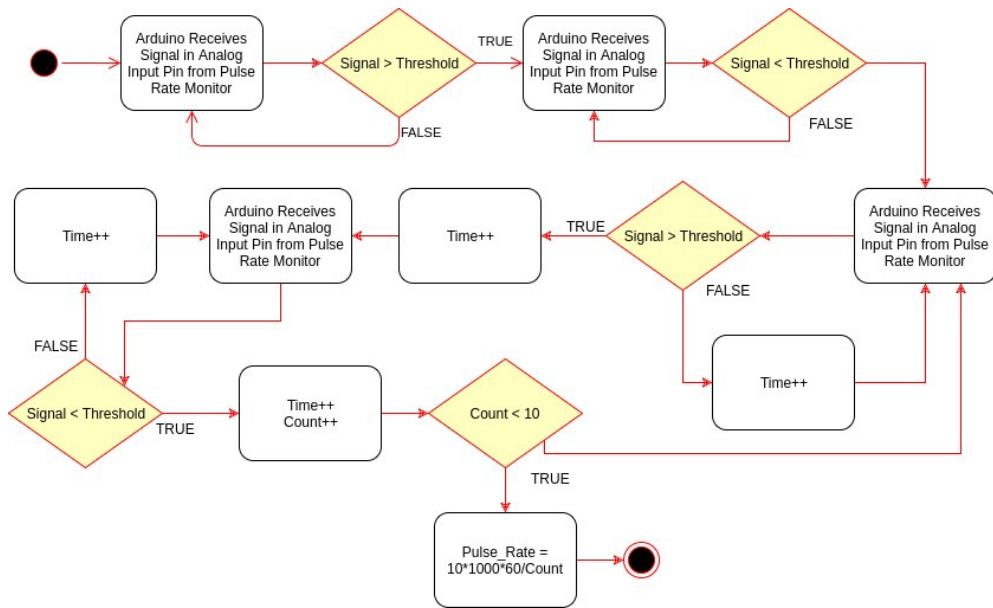
Figure 3.10: Algorithm used in the first pulse rate detector.

To illustrate how this device works, a simulation used five sinusoidal voltage sources to reconstruct the noisy PPG signal and applied it as an input to the circuit in LTspice (Figure 3.11(a)). The voltage sources used were: two to reconstruct the actual pulse wave, one to account for low frequency noise typical of movement artefacts, one to add high frequency noise and the last one to introduce 60Hz noise from the electrical grid. The simulation results in Figure 3.11(b) show the output to each part of the designed circuit and it is interesting to note that after the first stage it is already possible to see the user's pulse, but there's still some fluctuations that could complicate the calculations. Still in the same figure, it is possible to see that, although the filter's second stage (in red) already delivers a rather square wave, some disturbances remained. Also, the offset and amplitude of the signal were not appropriate for the Arduino, which justifies the use of the BJT Amplifier to digitise it. Since the user interface did not display the resulting wave, the loss of fidelity in the waveform was not of much importance.
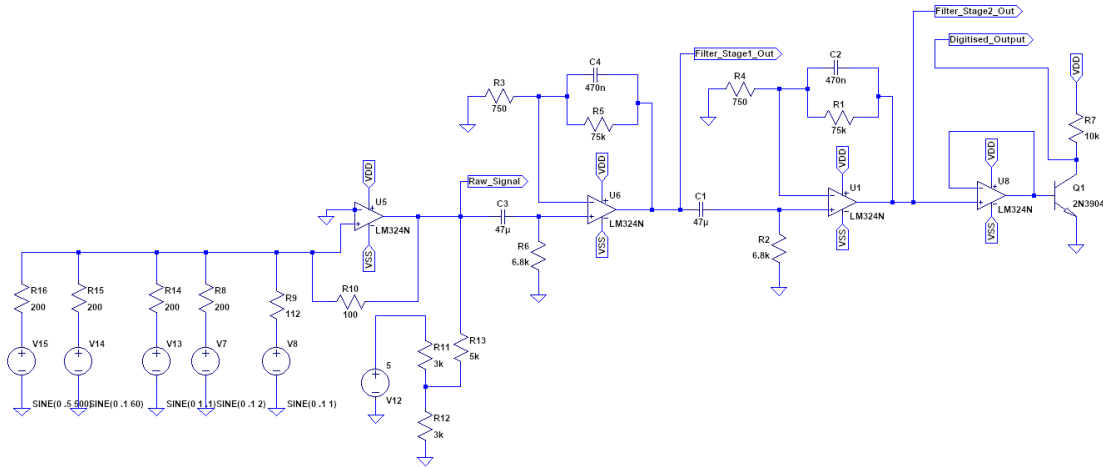
(a) Schematics used to simulate the pulse rate detector.
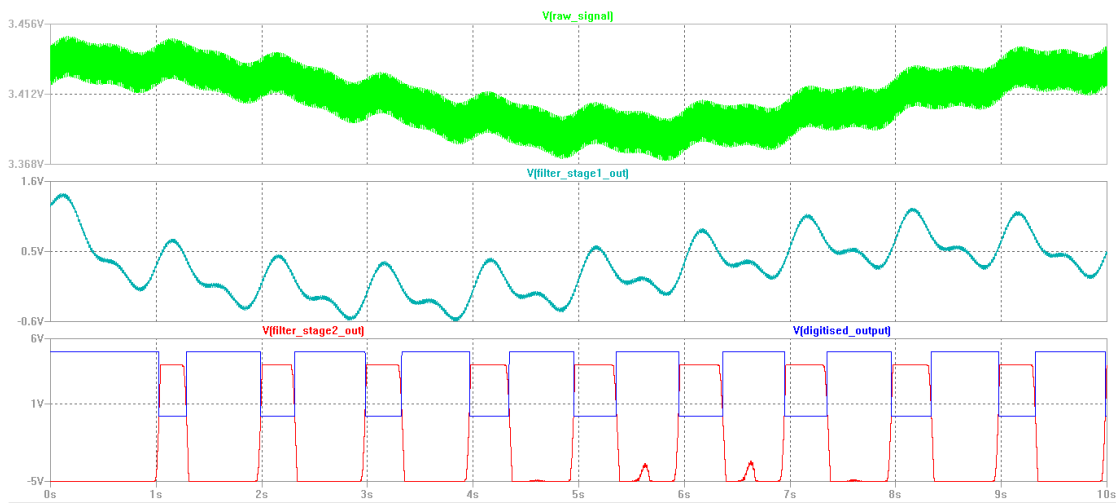
(b) Results from pulse rate detector simulation

Figure 3.11: Simulation of the pulse rate detector based on the Easy Pulse Project.

At a later opportunity, the design was improved with the aid of the University of Glasgow's lecturer, Dr. David Muir and Science Without Borders Student Carlos Meneghini. This version was built aiming at a graphic interface that would display the pulse wave plot, which entailed the need for a more complex algorithm. With that in mind, two bandpass filters with cut-off frequencies of 0.5Hz and 4.5Hz covering a range of 30BPM to 270BPM and a gain of 20.83dB each were designed (Figure 3.12(a)). It was expected that this design would be enough to eliminate any noise and fluctuations, but simulations confirmed that some small offset variations would remain (Figure 3.12(b)). If they were as small as the simulated results suggested, this would not have been an issue. However, after implementation, it was possible to see that the motion artifacts were indeed much bigger than anticipated (see Figure 3.13), which warranted some modifications.
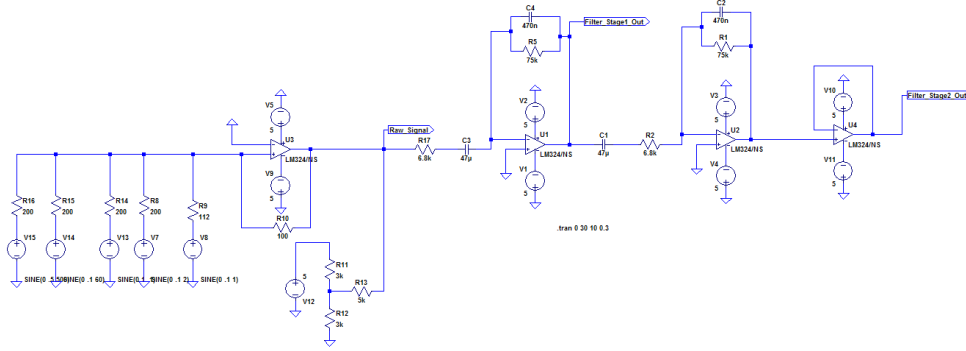
(a) Schematics for the first attempt at a new pulse rate detector design.
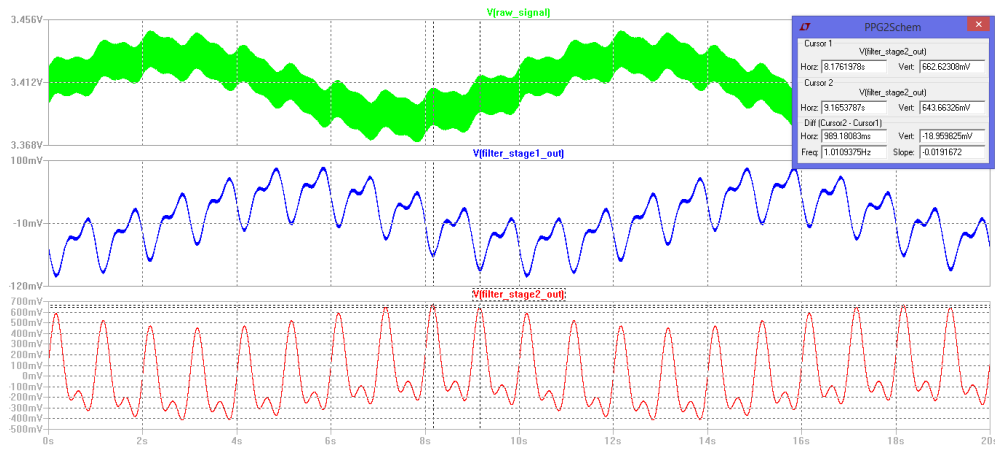
(b) Results from the new pulse rate detector design simulation.

Figure 3.12: First attempt at the new pulse rate detector simulation.
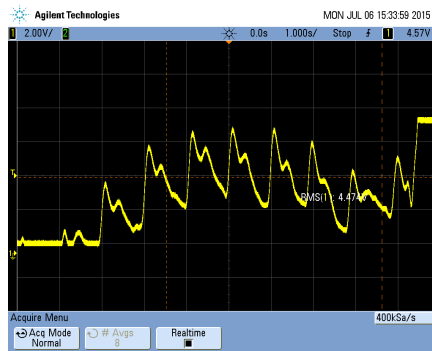
Figure 3.13: Results from first implementation of the new pulse rate detector with discrete components.

In order to mitigate these fluctuations, two measures were taken. Firstly, to diminish the mechanical displacement between the finger and the sensor, a set of sensor supports were designed (See Figure 3.14). Ideally, these supports would make the distance between the finger and the sensor constant, lowering the effect of movement in the signal. Also, a third low pass filter was used to increase the slope of the frequency response curve, resulting in the circuit from Figure 3.15.

(a) Cylindrical Ring Support

(b) Oval Ring Support

(c) Conical Ring Support

(d) Oval-Conical Ring Support
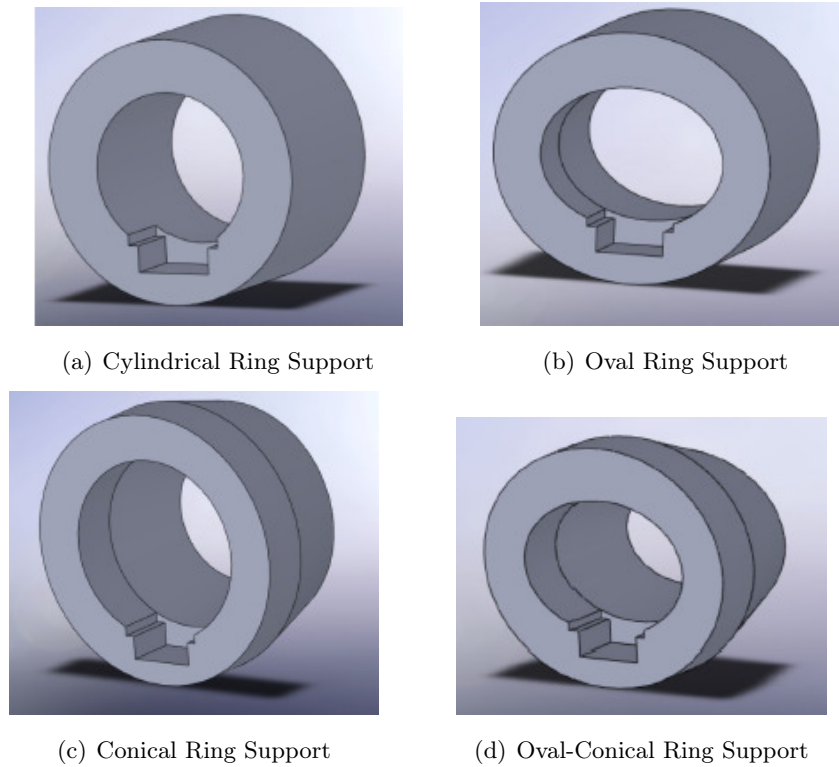
Figure 3.14: Sensor supports designed to mitigate motion artefacts.
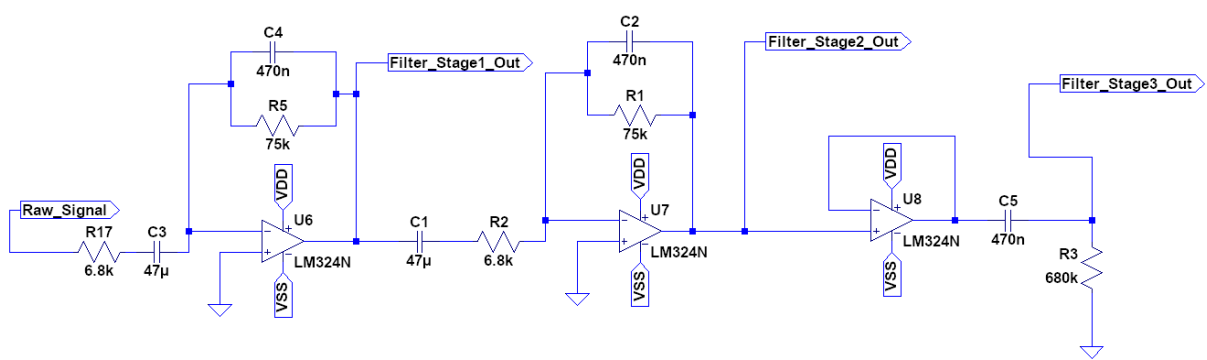
Figure 3.15: Final schematics for the new pulse rate detector.

Finally, the algorithm used to compute the heart rate can be seen in Figure 3.16. It is interesting to note that the first Pulse Rate Monitor was developed for an arduino, as the other modules, but the second version was designed for the Freedom Board (FRDM-KL25Z) due to the circumstances it was developed at. However, due to the similarities between these two prototyping platforms, the algorithm and the code were almost entirely compatible with the Arduino Platform.
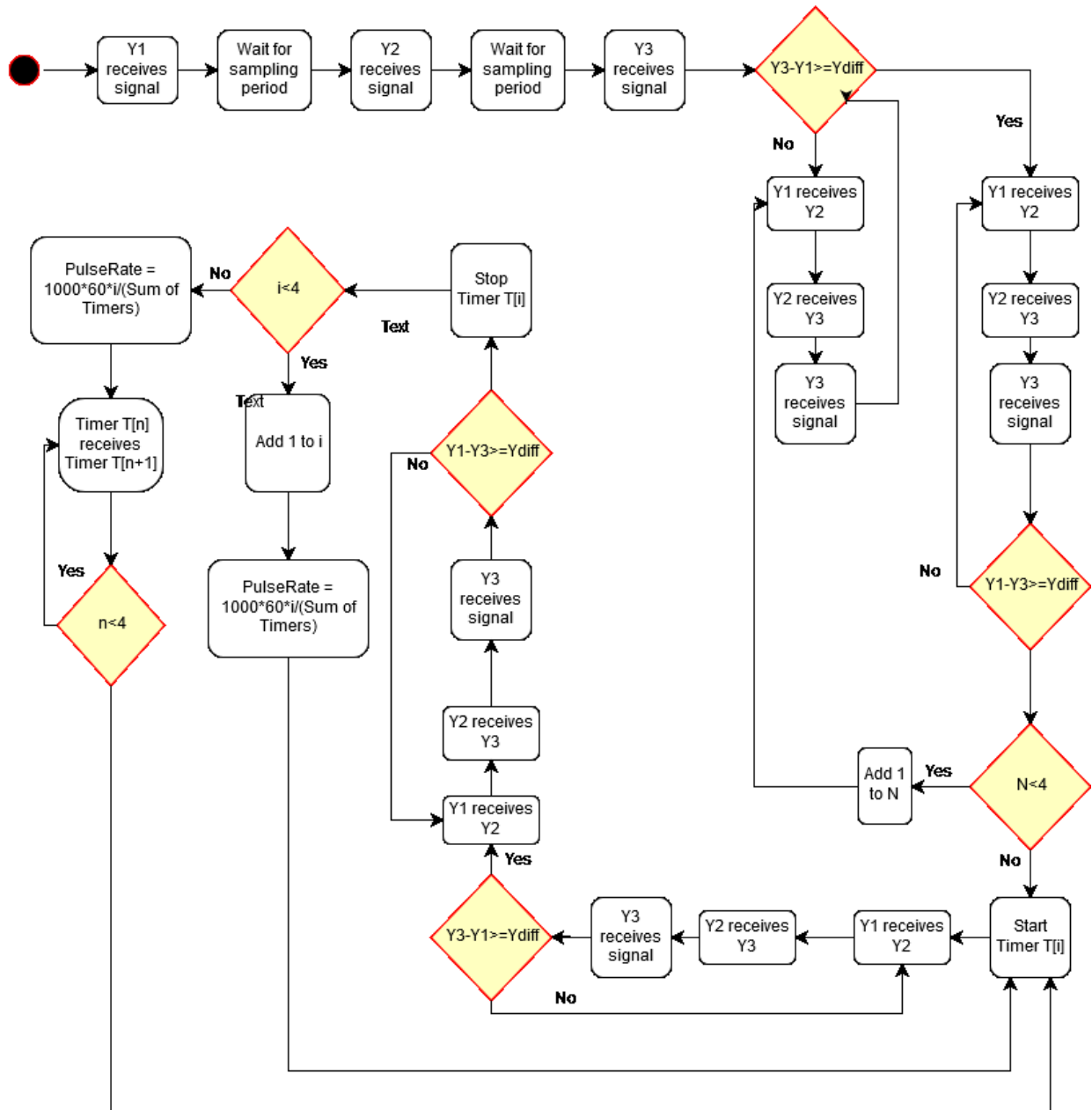
Figure 3.16: Algorithm used in the new pulse rate detector.

3.7 Bioimpedance Analysis

In order to achieve the specifications described in Chapter 2, the bioimpedance analysis device was divided into two modules: an oscillator (to deliver a sinusoidal signal with a 50kHz frequency)

and a current source (to regulate the current to ensure it would not be harmful to the user, and to ensure the human body would be subjected to a voltage big enough to provide accurate data regarding the bioimpedance). This section will detail the process that led to the current design.

3.7.1   The Current Source

The current source was designed to ensure that the current applied by the device would remain relatively constant and below any dangerous thresholds. With that in mind, the device was designned to maintain a current of aproximately $500\mu A$. The circuit in Figure 3.17 was used in order to achieve these specifications.
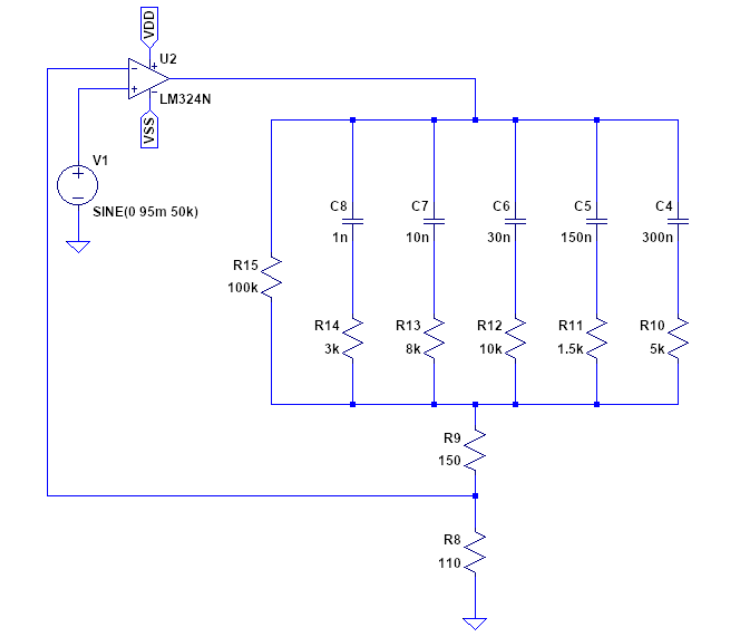
Figure 3.17: Schematics for the current source used by the **BIA** device.

This design attempts to maintain equal voltages in the two input terminals from the operational amplifier, which means that if a certain voltage is applied to V_+, the same voltage should be applied to the 110Ω resistor, thus creating a way to control the current flowing through the load. That way, for a sinusoidal current with an RMS value of $500\mu A$, a RMS voltage of 55mV must be applied to V_+.

3.7.2   The Oscillator

The design of the current source provided the value of the output voltage of the oscillator, which was the last specification needed to design the oscillator. Looking to fulfil the remaining needs, three designs were simulated and implemented until a working prototype was finally obtained.

3.7.2.1 Hartley Oscillator

Aiming at the low costs and low power dissipation, the first attempt at an oscillator used the Hartley topology. With very few components, this configuration provides a semi-sinusoidal signal, ideal for the device in question. Figure 3.18 shows this circuit 3.18(a) and the respective simulation results 3.18(b).
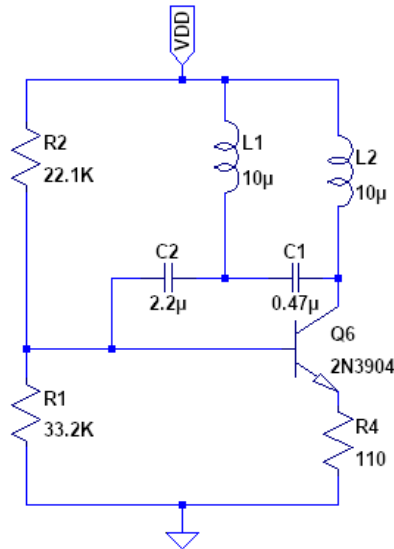
(a) Schematics for the simulation of the Hartley Oscillator.
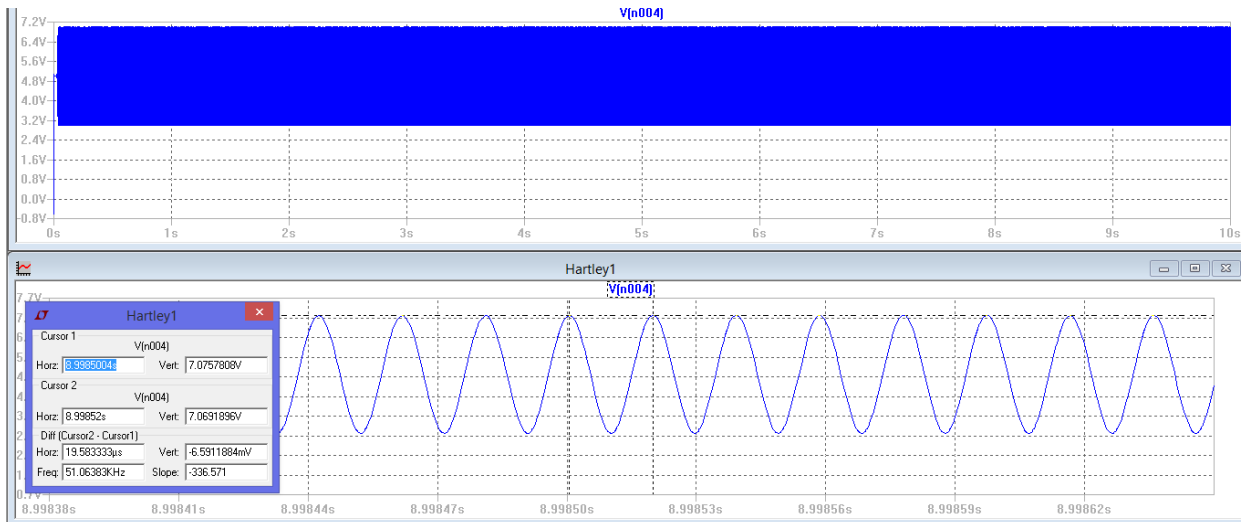
(b) Simulation results of the Hartley Oscillator

Figure 3.18: Simulation of the designed Hartley Oscillator.

3.7.2.2   Cross-Coupled Oscillator

As an alternative to the Hartley Oscillator, a Cross-Coupled Oscillator was also simulated. This topology consists of two tuned gain stages in a feedback loop as can be seen in Figure 3.19.
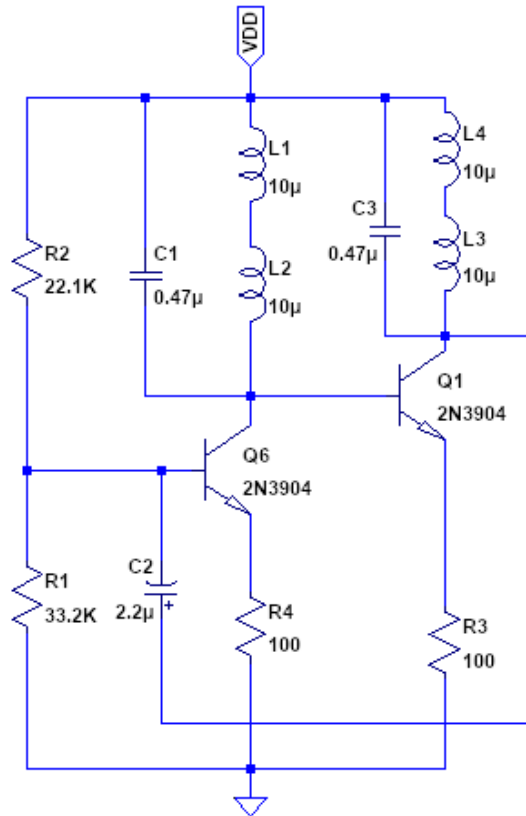
(a) Schematics for simulation of the Cross-Coupled Oscillator.
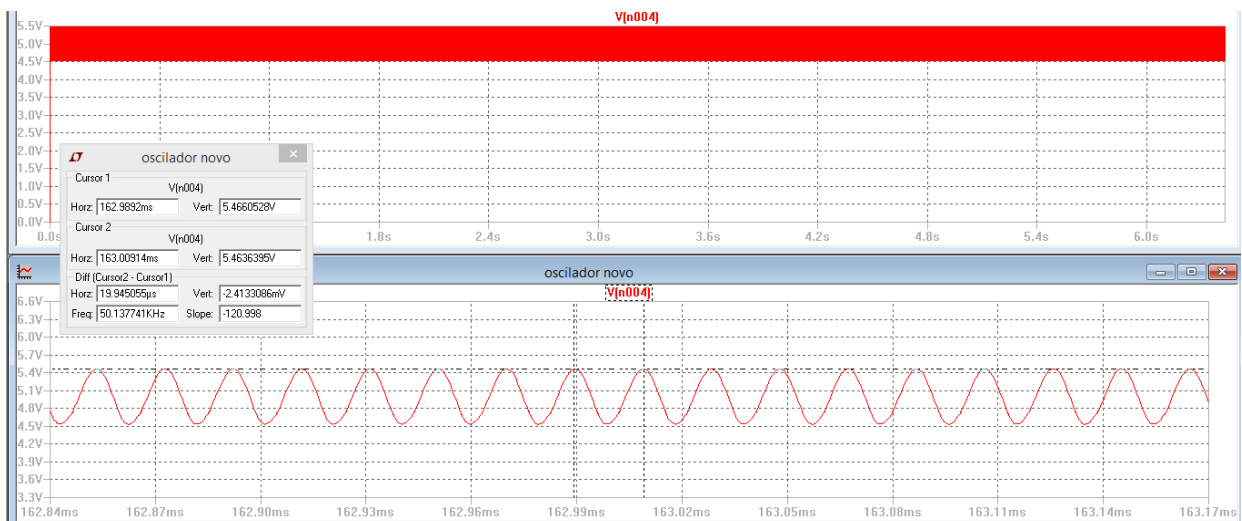
(b) Simulation results of the Cross-Coupled Oscillator.

Figure 3.19: Simulation of the designed Cross-Coupled Oscillator.

Even though this topology uses a few more components than the Hartley Oscillator, a comparison between the simulation results from the two circuits (Figure 3.20) showed that the Cross-Coupled Oscillator achieved the permanent regime faster.
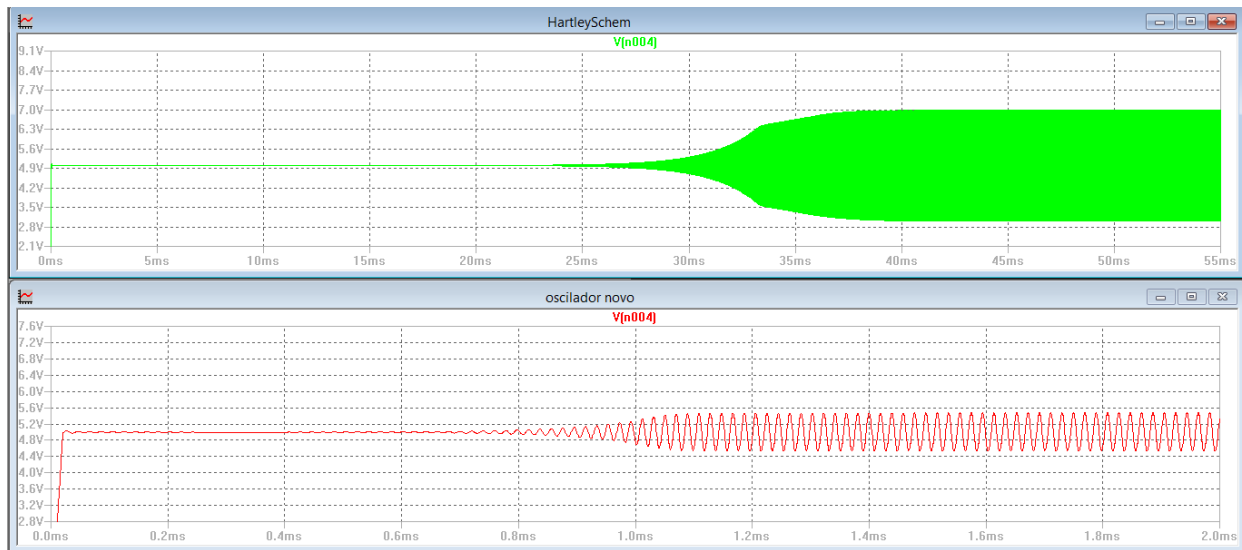
Figure 3.20: Comparison between the Hartley and the Cross-Coupled Oscillators on start up.

3.7.2.3 Relaxation Oscillator

Although the two previous topologies presented a relatively inexpensive and efficient approach to the problem, they proved to be very difficult to implement with discrete components, which led to the third oscillator design, the Relaxation Oscillator, also known as the Astable Multivibrator. The problem with this topology was that the output waveform would be a square rather than sinusoidal. This meant that frequencies other than the desired one would also be present, warranting then a set of filters. However, simulation (Figure 3.21(b)) of the resulting schematics (Figure 3.21(a)) showed that the intended frequency would be so big for that when compared to the operational amplifier oscillator, the resulting waveform resembled a triangular wave instead of the expected square wave.
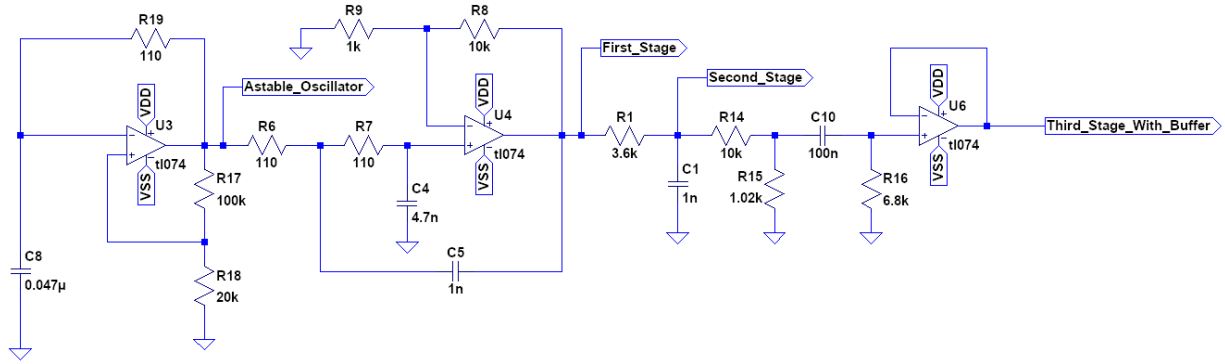
(a) Schematics for simulation of the Relaxation Oscillator.
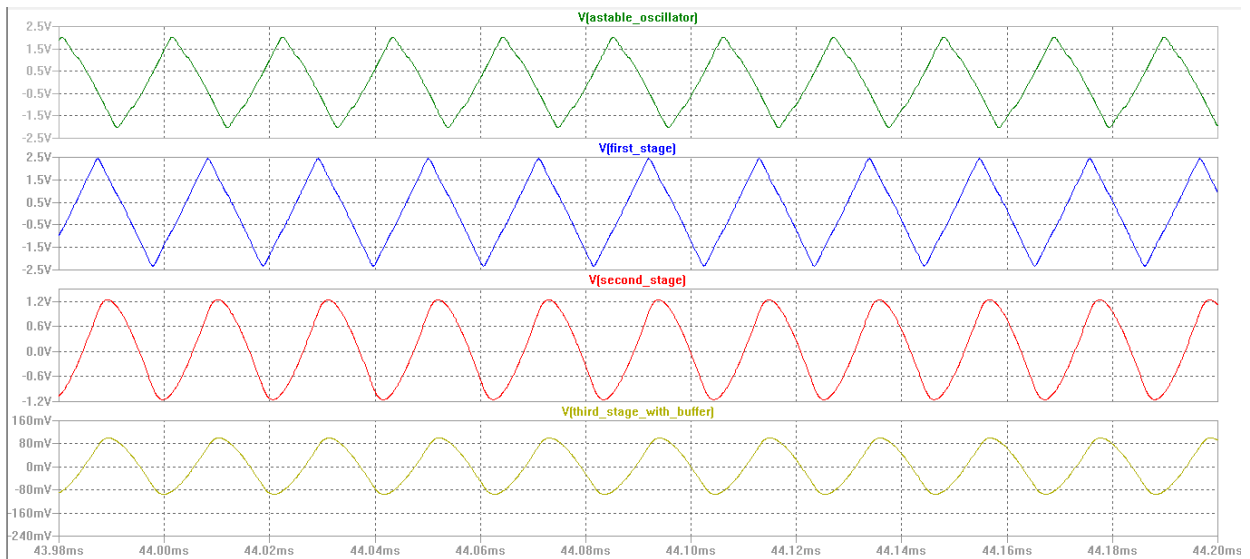
(b) Simulation results of the Relaxation Oscillator.

Figure 3.21: Simulation of the Relaxation Oscillator, also known as the Astable Multivibrator.

Differently from the other two, this oscillator was successfully implemented using discrete components and it presented satisfactory results that will be discussed in Chapters 4 and 5.

3.7.3 Bioimpedance Analysis Device

Upon completion of a working oscillator and the current source, a final design for the **BIA** device was assembled. The resulting circuit is shown in Figure 3.22. It is important to note that the physical implementation of the oscillator, although successful diverged a little from the simulation, and therefore, some adjustments were made to ensure the output would be compatible with the expected input to the current source.
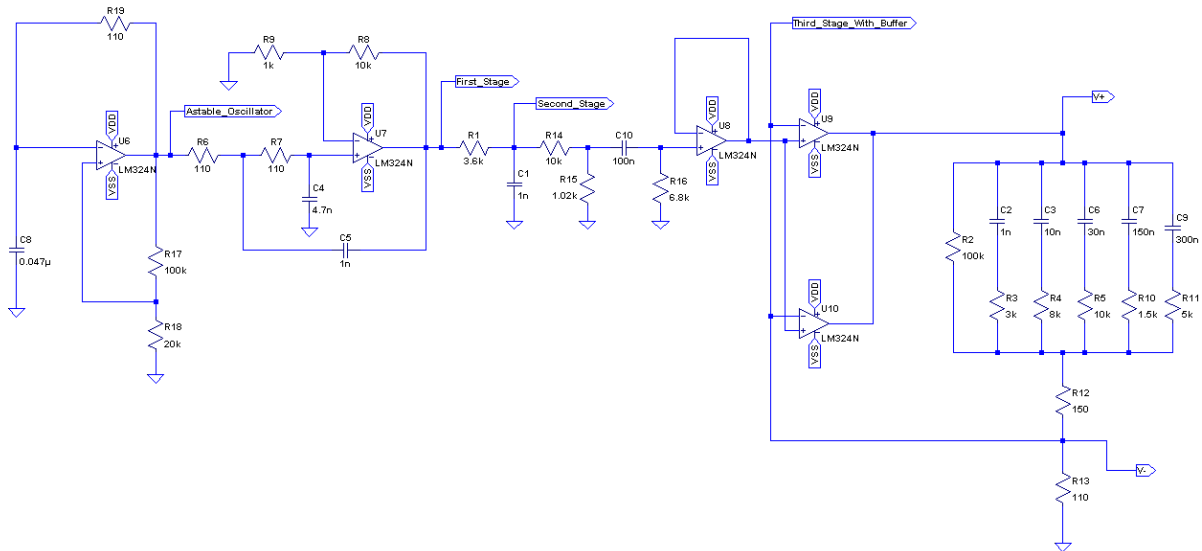
Figure 3.22: Complete schematic of the implemented BIA device using the Relaxation Oscillator and the current source with an equivalent circuit of the human body between the V_+ and V_- terminals.

3.8 Software

The software developed for this system can be divided into two parts. The arduino software monitors the user interface and the different sensors (except the weight scale ones) and sends data to the Java Application. The Java Application receives input from the Arduino, monitors the weight scale and provides a second user interface, where the recommendation is displayed.

As explained in section 3.3 the system works considering two situations: (i)when there is no user the system generates a general recommendation, and (ii)when there is a user the system generates a personalised recommendation. While the forward button is not pressed, the system remains in (i) and the Arduino sends to the Java Application the information about the environment so that a general recommendation can be generated. If the button is pressed once (ii), then the user interface will guide the user through the different biological measurements and sends them. Once they are all taken, they are sent to the Java Application and the personalised recommendation is displayed. This data flow is better illustrated by the flow diagram in Figure 3.23.
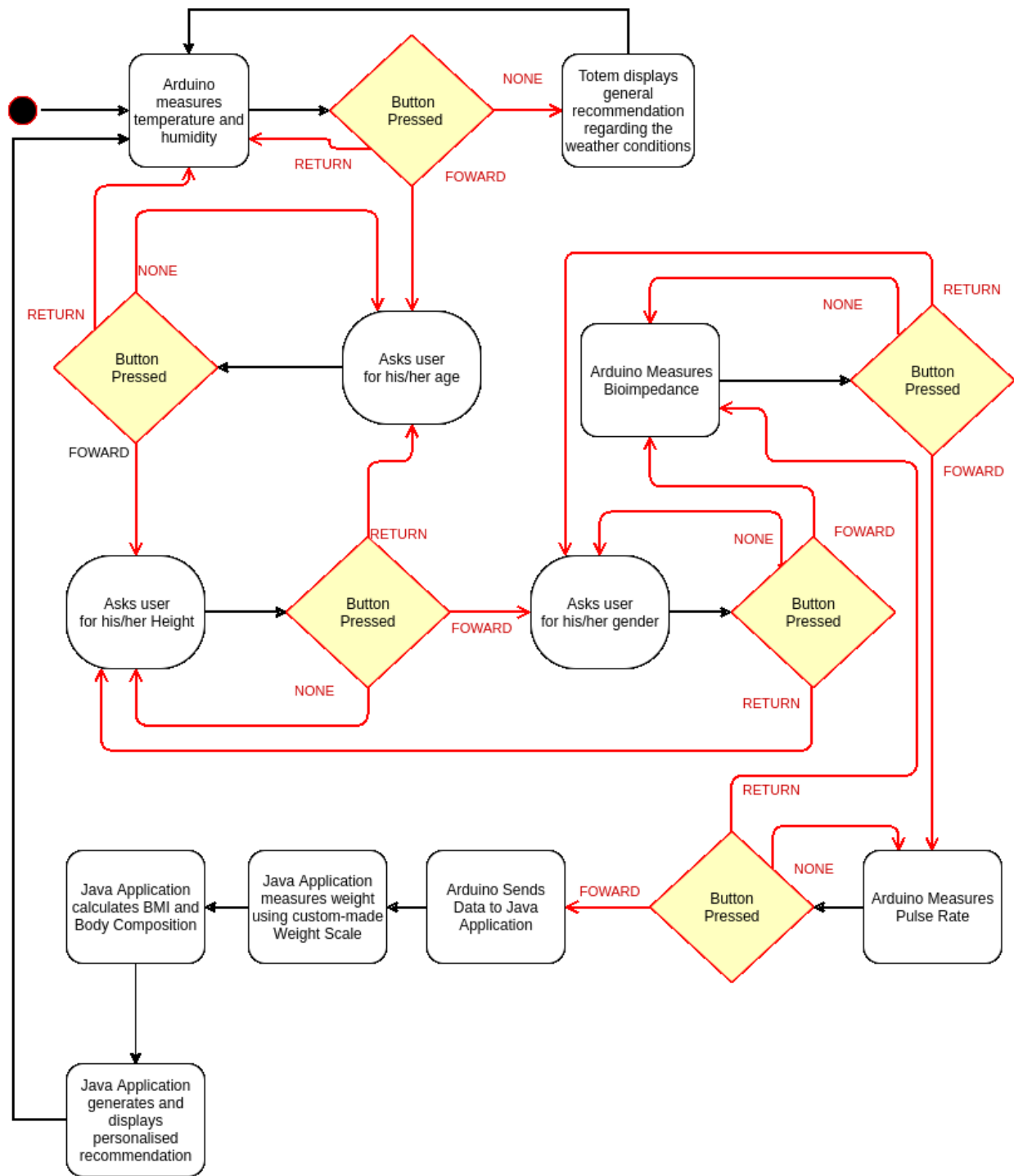
Figure 3.23: Flow Diagram describing the data flow inside the system.

The Java application is divided into four packages. The main package is where the main class is located. The "model" package is where classes that model the physical entities of the system are stored. In it, the classes "Arduino", "Person" and "PhidgetBridge" can be found. The "user interface" package gathers the different graphic interfaces developed for different situations, depending on which platform the system was running. The "Utilities" package contains classes classes that

assist the system such as the random data generator, for simulations, the SQL communications, to store the simulation results in a database, and the recommendations class, which holds the production rules that define which recommendation will be given.

When the system starts, the main class creates an object from the "Arduino" class which will then either generate random data for a simulation, or communicate with the Arduino to collect real data, depending on how it is initially set.

If the system is set to read real data, the object instantiated from the "Arduino" class will then generate a "Person" instance and fill it with the data received from the Arduino. In case it is set to simulation, it will generate all of the data and fill the "Person" object with it. This class also generates the communication with the Phidget bridge through a "PhidgetBridge" object.

Once all of the data is either obtained or randomly generated, the "Arduino" object calls the user interface, which will assess whether or not it has enough information for a personalised recommendation and act accordingly.

This flow is better illustrated in Figure 3.24.
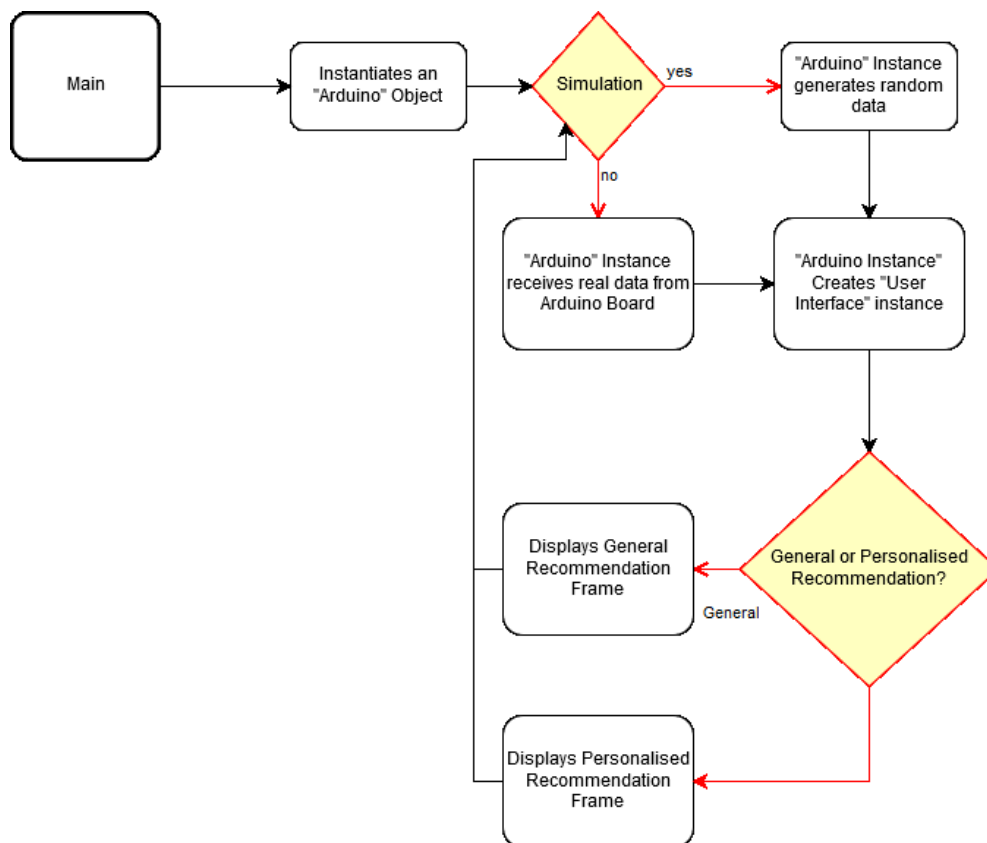
Figure 3.24: Flow Diagram describing the Java Application.

Chapter 4

Experimental Results

4.1 Introduction

Even though the experiments detailed in this chapter were intended to provide a proof of concept for the system described in this monograph, the sections below will only cover experiments performed on the Pulse Rate Monitor (Section 4.2) and the Bioimpedance Analysis Acquisition module (Section 4.3). The reason for such choice is that the remaining blocks were a direct implementation of commercial devices and as such they were not thoroughly tested.

4.2 The Pulse Rate Monitor

In order to assess the quality of the designed pulse rate monitor a three-stage experiment was performed. Initially, the intended design was simulated to model the behaviour of the filters. Then, it was implemented a prototype with discrete components and the results were compared to the simulations. After that, the necessary adjustments were made and a printed circuit board was built (Figure 4.1). With the PCB in hand and the algorithm implemented, the pulse rate measurements taken with this prototype were then compared with three other systems for three subjects.
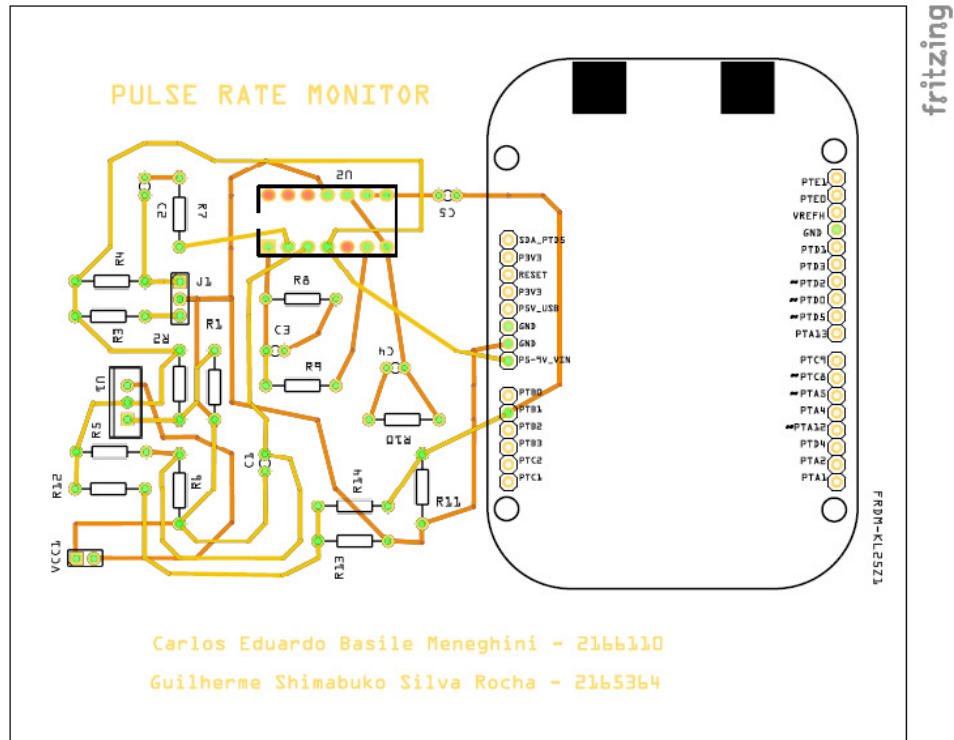
Figure 4.1: PCB design for the Pulse Rate Monitor

The first simulation provided data on what to expect from the filter's behaviour, and indicated that the design was appropriate for the application at hand. However, as described in Chapter 3, after the first attempt at a physical implementation, it was noticed that the fluctuations seen in the simulation were much bigger than anticipated, so a third stage filter was implemented. Figure 4.2 is a comparison between the simulations and the final physical implementation before and after the third stage was included.

In Figure 4.3 it can be observed that the third stage maintains the gain in the signal's typical frequencies and that it is an effective way of eliminating the low frequency fluctuations aforementioned.
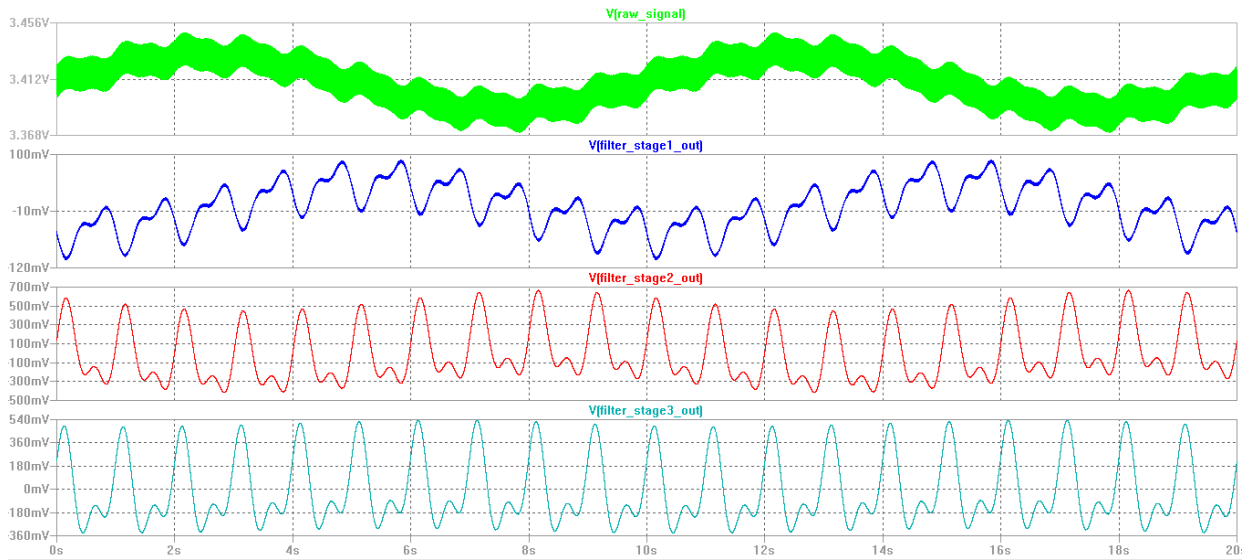
(a) Pulse Rate Detector Final Simulation.
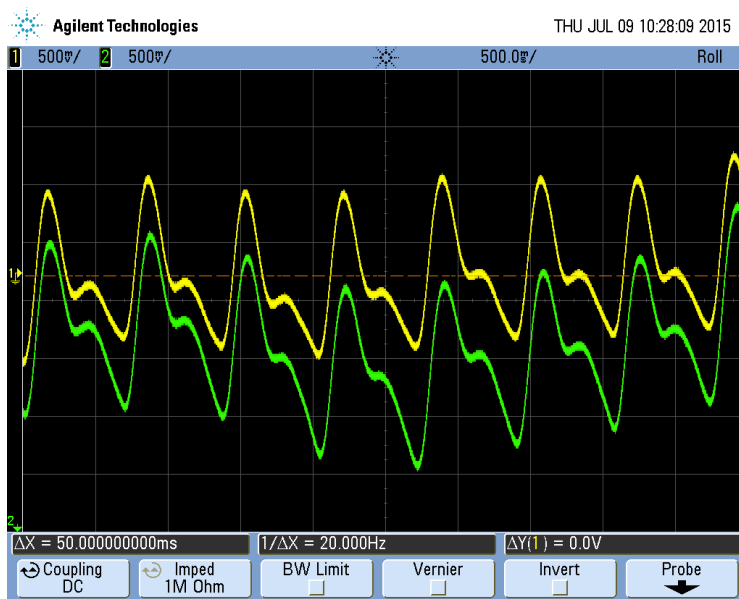
(b) Pulse Rate Detector PCB Test Showing Filter's Second and Third
Stages.

Figure 4.2: Comparison between simulation and tests on the PCB for the Pulse Rate Monitor.
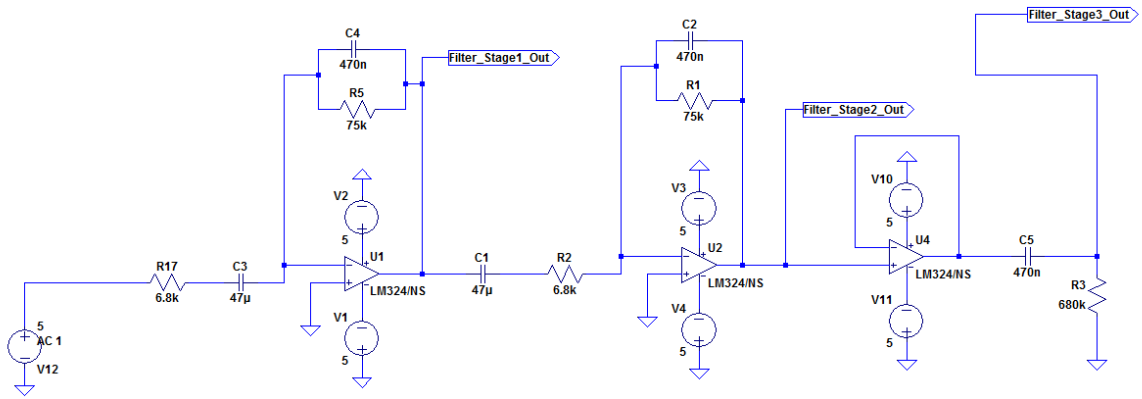
(a) Schematics for simulation.
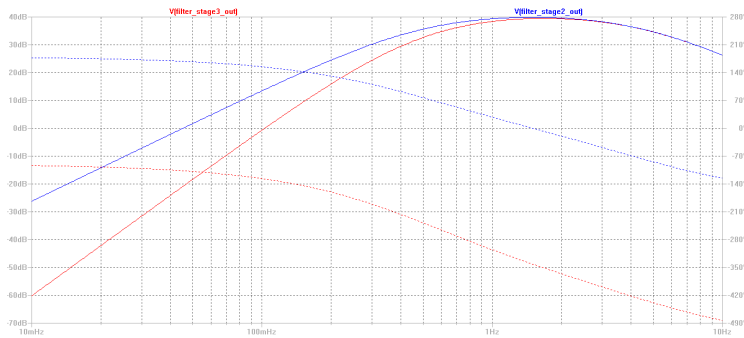
(b) Simulation results.

Figure 4.3: Frequency response analysis showing the change in steepness during the low frequencies before and after the third stage was implemented.

The system in question was then compared with three other systems. The first one used the "Polar H7 Bluetooth 4.0 Heart Rate Sensor"and its application, "Polar Beat". The Polar H7 Heart Rate sensor is a belt, meant to be worn around the chest area, with two electrodes that measures the heart rate. Secondly, an android application, "Instant Heart Rate", which uses a smartphone's camera and flash light to measure the heart rate was used. Lastly, the native heart rate monitor from the Samsung Galaxy S5, that also uses an inbuilt reflective optical sensor, was tested. As Table 4.1 indicates, the measurements from all sensors were relatively similar, always maintaining a deviation smaller than two standard deviations.

Table 4.1: Values obtained from three subjects using 4 different systems.

	Polar Beat	Instant Heart Rate	S Health	Developed System	Mean	Standard Deviation	Biggest Deviation From Mean
Subject 1	64	65	63	62	63.5	1.29	1.5
Subject 2	76	79	76	74	76.25	2.06	2.75
Subject 3	97	100	102	99	99.5	2.08	2.5

Figures 4.4, 4.5 and 4.6 shows the pulse rate monitor measurements from the experiments summarized in Table 4.1 with the new graphic interface.
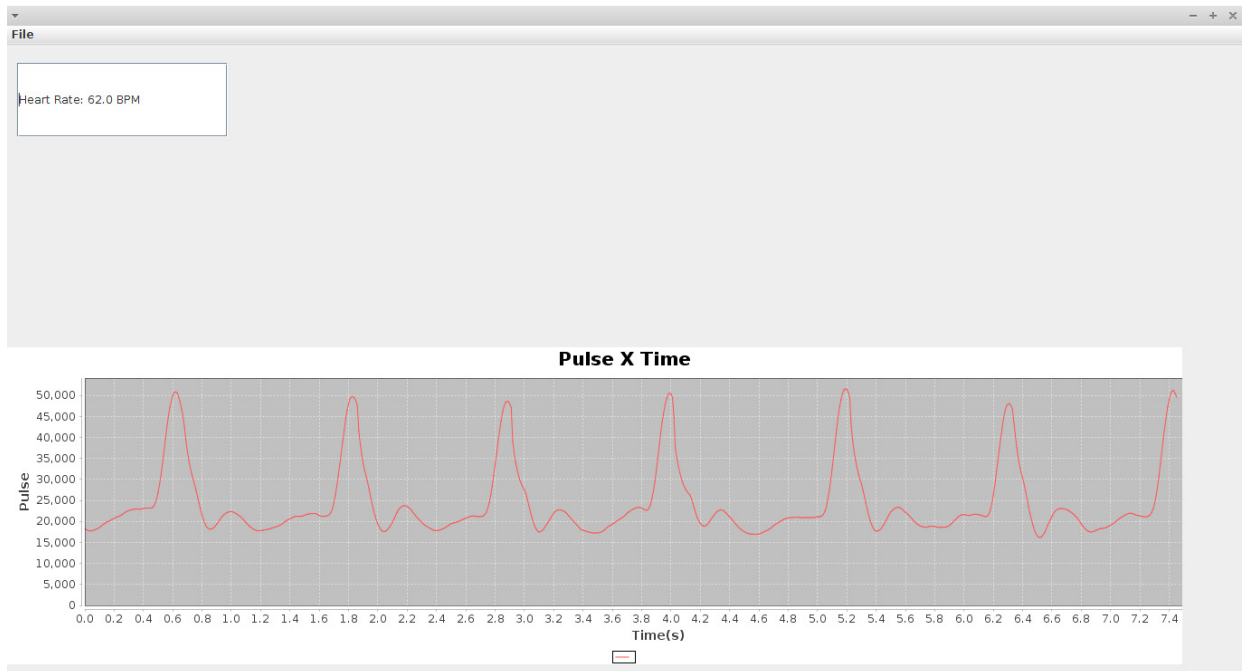
Figure 4.4: Pulse Rate Monitor for subject 1.
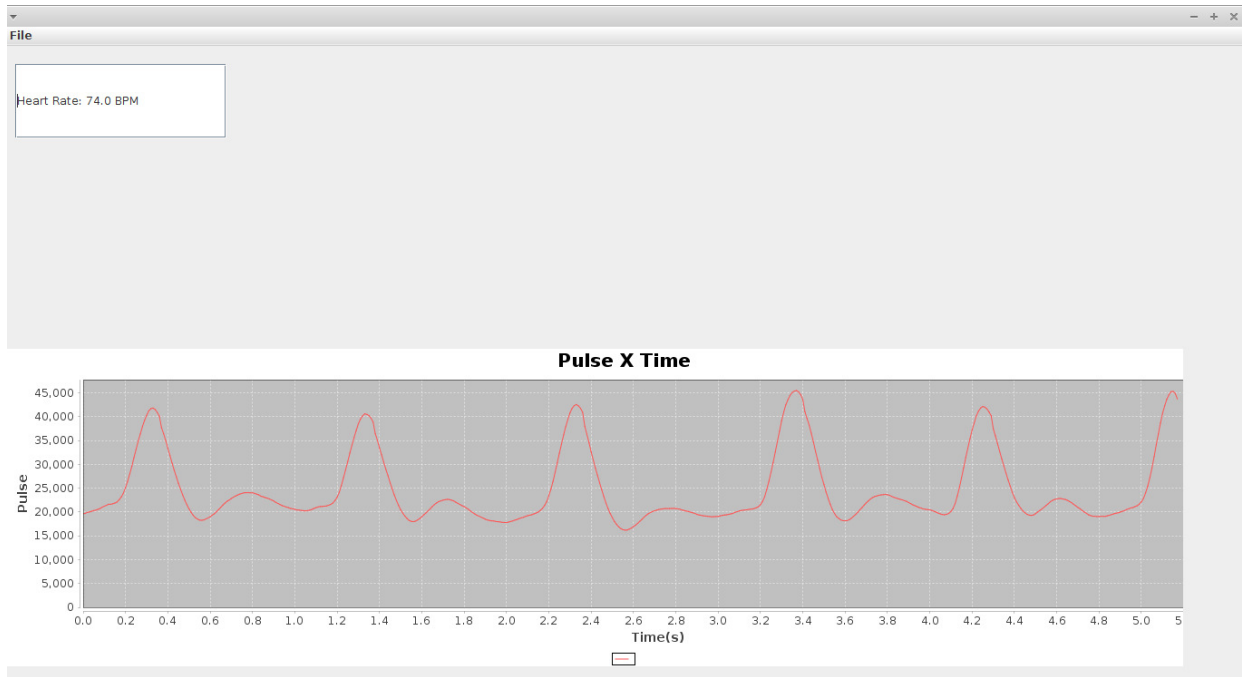
Figure 4.5: Pulse Rate Monitor for subject 2.
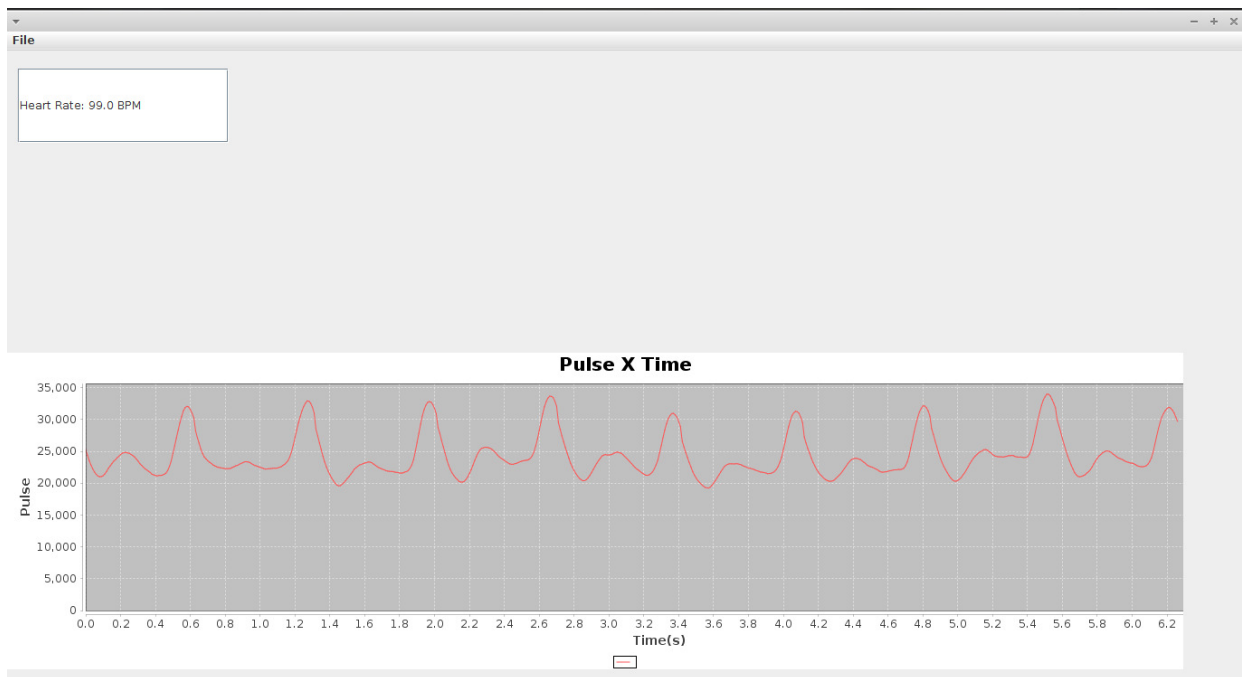
Figure 4.6: Pulse Rate Monitor for subject 3.

4.3 The Bioimpedance Analysis Device

The experiments designed to validate the BIA device were aimed at the capacity of the device to measure the impedance of the human body and to regulate the current so that it does not pose a threat to the user. To safely assess these characteristics, three experiments were created. As mentioned in Chapter 2, the typical bioimpedance ranges from 250Ω to 300Ω, and to be properly validated, the device should work with impedances as high as $1000 - j500\Omega$. With that in mind, the first test was made by measuring a varying a resistive load from 110Ω to 1100Ω with a 110Ω step. The resistors used have a tolerance of 1% in its nominal value, and the measurements were made using an oscilloscope with a $0.1mV$ accuracy. Figure 4.7 is a plot of the nominal value of the load, with error bars representing the tolerance of this value, and the resistance estimation from the measured values with error bars representing the propagated error from the oscilloscope readings. This plot shows that for this experiment with purely resistive loads varying within the recommended range, the device could be used to accurately estimate the loads.
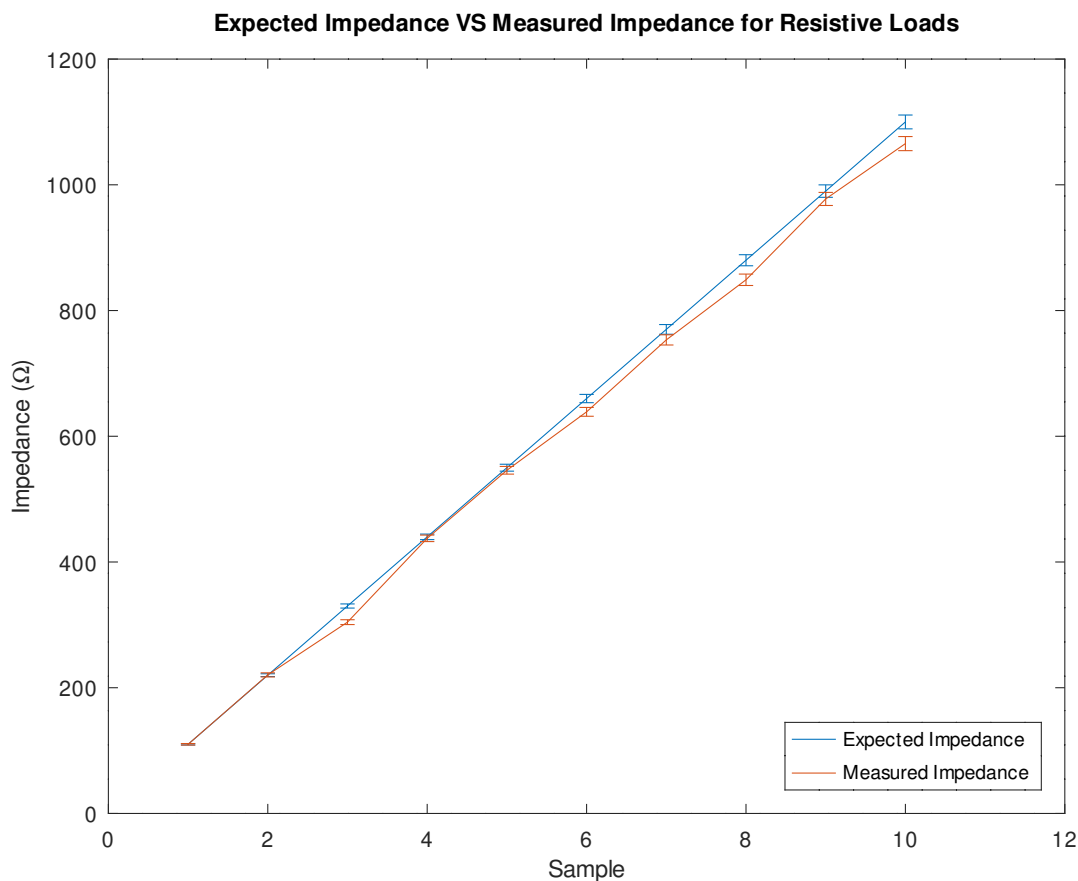
Figure 4.7: Experimental results for the BIA device using purely resistive loads.

Table 4.2 shows the data collected without taking the resistor tolerance or the oscilloscope's error propagation into consideration. The average error was calculated using equation 4.1 resulting in an average error of 2.6% and a maximum of 7.78%, while maintaining satisfactory values of

current (I<500μ).

$$Error(\%) = \frac{|R_{nominal} - R_{measured}|}{R_{nominal}} \times 100 \tag{4.1}$$

Table 4.2: Table displaying the results of the trials for the **BIA** device using purely resistive loads.

$R_{nominal}(\Omega)$	$V_1(mV)$	$V_2(mV)$	$\mathbf{I}(\mu)\mathbf{A}$	$R_{measured}(\Omega)$	**Error**
110	90.20	45.10	410	110	0%
220	152.00	50.60	460	220.43	0.2%
330	200.00	53.10	482.73	304.31	7.78%
440	232.00	46.60	423.64	437.64	0.54%
550	288.00	48.30	439.09	545.90	0.75%
660	322.00	47.30	430	638.84	3.21%
770	372.00	47.40	430.91	753.29	2.17%
880	401.00	46.00	418.18	848.91	3.53%
990	435.00	44.0	400.00	977.50	1.26%
1100	498	46.60	423.64	1065.54	3.13%

Following that test, it was necessary to see how the device would behave with a load that held a better resemblance to the human body. For that, the equivalent circuit from Figure 2.1 from Chapter 2, was used. In this circuit, the resistance from the parallel branch was varied at a 110Ω step with an initial value of 110Ω up to a resistance of 1210Ω and the capacitance was first varied with a 2ηF with an initial value of 1ηF up to a final capacitance of 9ηF. As the experiment progressed, it was noticed that for bigger values of resistance, the capacitance didn't need to change that much to reach reactance values of 500Ω, so the step and the variation changed for the capacitance as to limit the reactance value to the range of interest. Later, one last measurement was made to cover one case in which the resistance would be over 1000Ω and the reactance would be bigger than 500Ω. The nominal values are computed according to equation 4.4 as follows.

$$R_{equivalent}\Omega) = R_s + \frac{R_p}{1 + (2\pi\omega R_p C_p)^2} \tag{4.2}$$

$$X_{equivalent}\Omega) = -\frac{2\pi\omega C_p R_p^2}{1 + (2\pi\omega R_p C_p)^2} \tag{4.3}$$

$$ExpectedImpedance(\Omega) = \sqrt{R_{equivalent}^2 + X_{equivalent}^2} \tag{4.4}$$

Then, the expected impedance calculated with the nominal values were compared with the impedance measured with the oscilloscope using the BIA device. Figure 4.8 shows a plot of both the measured impedance and the expected impedance, with oscilloscope's error propagation and error from the resistor's tolerance. As the plot shows, both curves are nearly identical for most samples. The largest discrepancies occur for impedances greater than 800Ω. The resulting data is available in Table 4.3.
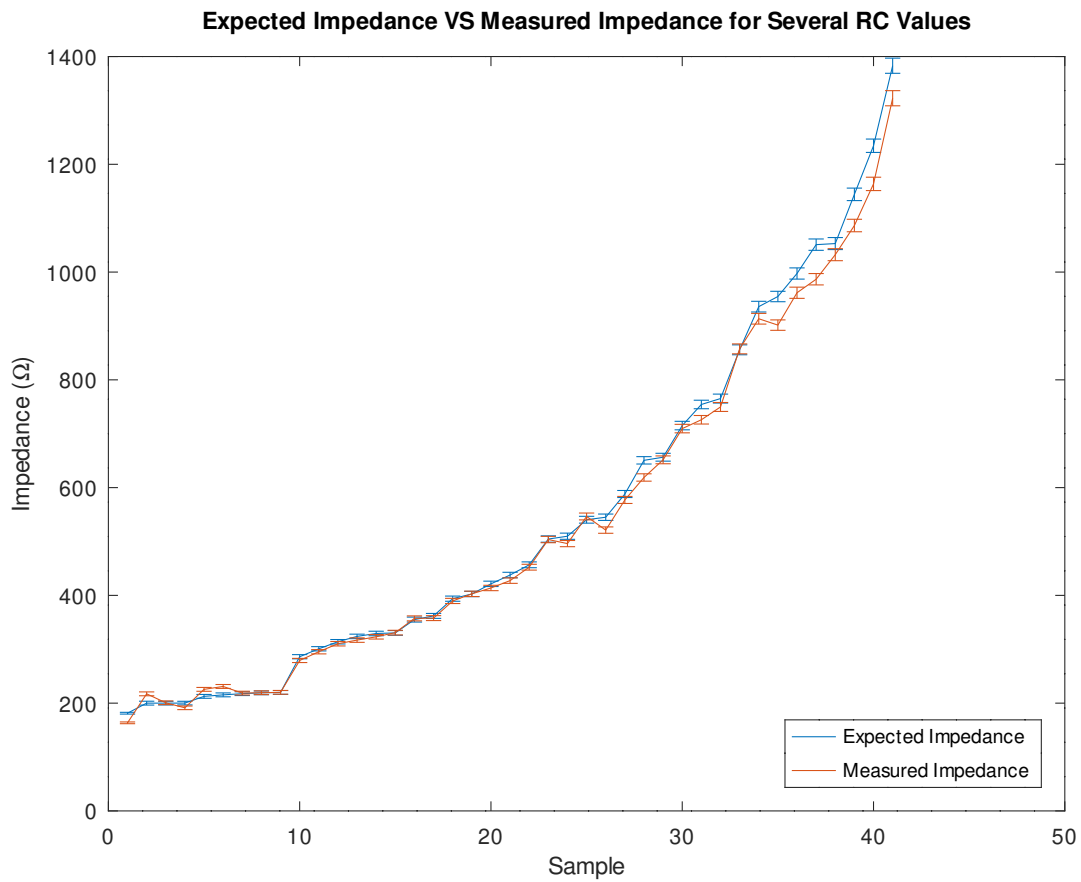
Figure 4.8: Experimental results for the BIA device using RC loads according to equivalent circuit in Figure 2.1 from Chapter 2

Table 4.3: Test results from first trial with RC equivalent circuit shwon in Figure 2.1.

$R_{1nominal}(\Omega)$	$C_{1nominal}(\eta F)$	$R_{eq}(\Omega)$	$X_{eq}(\Omega)$	$|z_{nominal}|(\Omega)$	$\dfrac{R_{nominal}}{|z_{nominal}|}$	$V_1(mV)$	$V_2(mV)$	$I(\mu A)$	$|z_{measured}|(\Omega)$	Error
110.00	1	219.87	-3.80	219.90	99.99%	135.00	44.99	409.00	220.07	0.08%
110.00	3	218.83	-11.28	219.12	99.87%	136.17	45.48	413.45	219.35	0.10%
110.00	5	216.81	-18.46	217.60	99.64%	134.68	45.08	409.82	218.63	0.48%
110.00	7	213.92	-25.14	215.39	99.32%	137.26	44.28	402.55	230.98	7.24%
110.00	9	210.30	-31.19	212.60	98.92%	136.10	44.61	405.55	225.60	6.11%
110.00	25	172.99	-54.42	181.34	95.39%	108.53	43.65	396.82	163.50	9.84%
220.00	1	328.95	-15.13	329.30	99.89%	186.41	47.34	430.36	323.15	1.87%
220.00	3	320.93	-43.74	323.90	99.08%	181.33	46.71	424.64	317.02	2.12%
220.00	5	306.53	-67.92	313.96	97.63%	176.55	46.21	420.09	310.27	1.18%
220.00	7	288.27	-86.25	300.90	95.80%	171.93	46.65	424.09	295.41	1.82%
220.00	9	268.62	-98.67	286.17	93.87%	162.80	46.01	418.27	279.22	2.43%
330.00	1	436.49	-33.85	437.80	99.70%	231.76	47.44	431.27	427.39	2.38%
330.00	3	410.89	-93.58	421.42	97.50%	218.16	45.82	416.55	413.74	1.82%
330.00	5	370.11	-134.83	393.90	93.96%	204.55	45.03	409.36	389.68	1.07%
330.00	7	326.16	-156.87	361.92	90.12%	189.21	44.49	404.45	357.82	1.13%
330.00	9	286.42	-164.60	330.35	86.70%	177.03	44.17	401.55	330.87	0.16%
440.00	1	541.75	-59.68	545.03	99.40%	271.00	47.23	429.36	521.17	4.38%
440.00	3	485.44	-155.69	509.79	95.22%	247.13	44.85	407.73	496.12	2.68%
440.00	5	407.76	-205.80	456.75	89.27%	223.70	43.76	397.82	452.32	0.97%
440.00	7	337.24	-219.88	402.59	83.77%	203.18	43.58	396.18	402.85	0.06%
440.00	9	282.70	-214.86	355.08	79.62%	185.28	43.61	396.45	357.34	0.64%
550.00	1	644.06	-92.28	650.63	98.99%	309.61	46.73	424.82	618.81	4.89%
550.00	3	543.51	-224.72	588.14	92.41%	271.60	43.48	395.27	577.12	1.87%
550.00	5	424.94	-272.08	504.58	84.22%	239.04	42.85	389.55	503.64	0.19%

660.00	1	742.79	-131.21	754.29	98.48%	341.51	44.94	408.55	725.92	3.76%
660.00	3	585.87	-296.01	656.40	89.25%	292.09	42.19	383.55	651.55	0.74%
660.00	5	428.10	-329.79	540.40	79.22%	245.16	41.08	373.45	546.47	1.12%
770.00	1	837.43	-175.97	855.72	97.86%	391.83	44.55	405.00	857.48	0.21%
770.00	3	614.37	-366.03	715.14	85.91%	304.20	40.83	371.18	709.54	0.78%
880.00	1	927.52	-226.01	954.66	97.16%	397.09	43.18	392.55	901.58	5.56%
880.00	3	631.37	-432.41	765.25	82.50%	314.64	40.26	366.00	749.67	2.04%
990.00	1	1,012.68	-280.75	1,050.88	96.37%	420.34	42.16	383.27	986.71	6.11%
990.00	2	823.81	-444.01	935.85	88.03%	365.63	39.30	357.27	913.39	2.40%
1,100.00	1	1,092.65	-339.58	1,144.20	95.49%	438.43	40.31	366.45	1,086.41	5.05%
1,100.00	2	854.41	-514.50	997.35	85.67%	380.33	39.04	354.91	961.63	3.58%
1,210.00	1	1,167.23	-401.89	1,234.48	94.55%	453.42	39.16	356.00	1,163.65	5.74%
1,210.00	2	876.79	-582.97	1,052.91	83.27%	391.28	37.68	342.55	1,032.27	1.96%
1,400.00	1	1,283.08	-515.95	1,382.93	92.78%	491.00	37.70	342.73	1,322.63	4.36%

However, after this data was analysed, it was noticed that even though the impedance of the load was increasing, the characteristic of the load was too dissimilar to that of the human body for many samples. To rectify this mistake, a new set of samples were measured. This time, the impedance module was increased from 200Ω to 1400Ω at a 100Ω step and for each value of impedance the resistance and the capacitance were adjusted to test loads with an 85% resisitive characteristic, a 90% resistive characteristic and a 95% resistive characteristic. Figure 4.9 shows the plots for both the nominal and the experimental impedances for each of these cases. These plots also corroborate that the measurements are more accurate for impedances smaller than 800Ω. They also indicate that the increase in reactive components also meant an increase in the deviation for larger impedances.
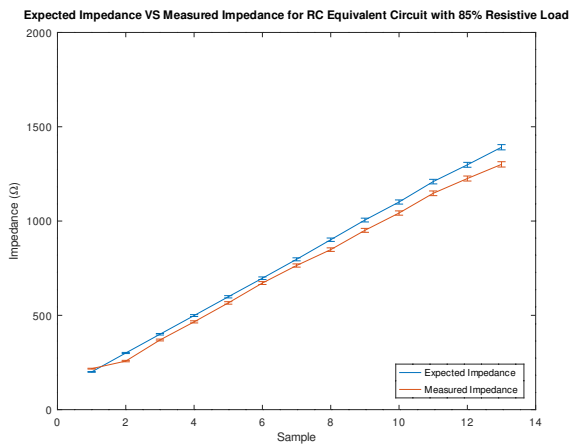
(a) RC Circuit with 85$ resistive load
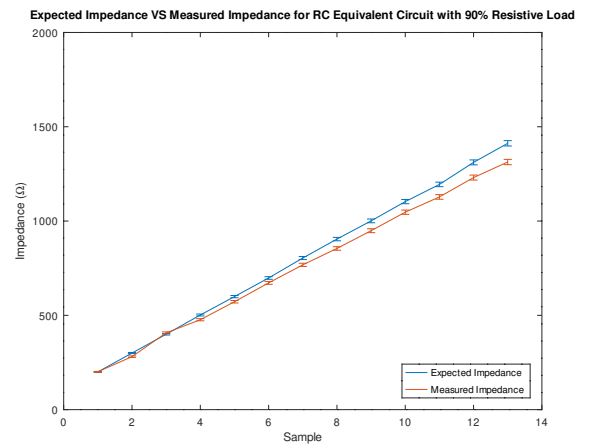
(b) RC Circuit with 90$ resistive load
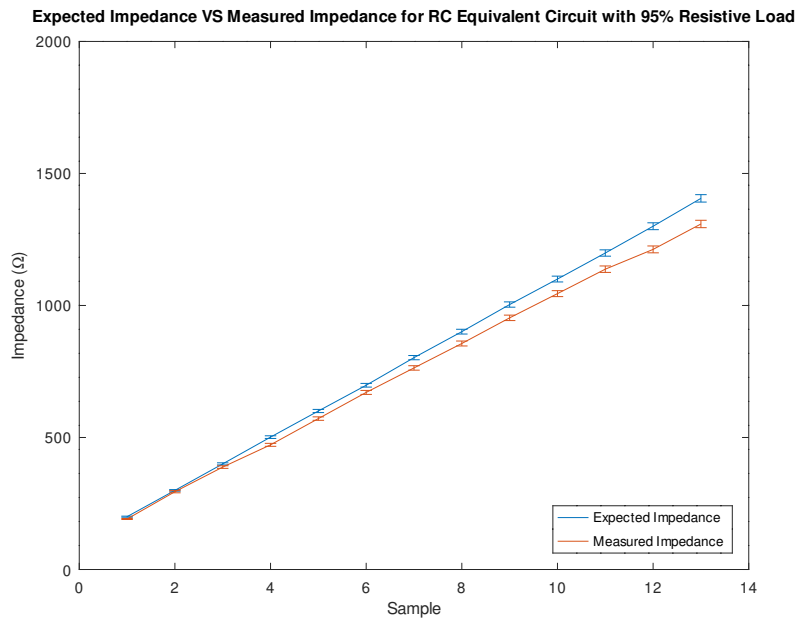
(c) RC Circuit with 95$ resistive load

Figure 4.9: Sensor supports designed to mitigate motion artefacts.

The data used to generate these plots can be seen in Table 4.4.

Table 4.4: Test Results from second trial with RC equivalent circuit shown in Figure 2.1.

$R_{1nominal}(\Omega)$	$C_{1nominal}(\eta F)$	$R_{eq}(\Omega)$	$X_{eq}(\Omega)$	$|z_{nominal}|(\Omega)$	$\frac{R_{nominal}}{|z_{nominal}|}$	$V_1(mV)$	$V_2(mV)$	$I(\mu A)$	$|z_{measured}|(\Omega)$	Error
129.00	19.3	190.07	-62.59	200.11	94.98%	121.87	44.49	404.45	191.32	4.39%
179.00	22.2	179.96	-87.34	200.04	89.96%	126.54	44.80	407.27	200.70	0.33%
245.00	22.8	170.01	-105.37	200.02	85.00%	128.03	43.03	391.18	217.29	8.64%
225.00	7.60E	284.61	-93.80	299.67	94.97%	160.00	43.50	395.45	294.60	1.69%
267.00	9.74	270.12	-130.82	300.13	90.00%	155.00	43.60	396.36	281.06	6.36%
317.00	10.9	255.52	-157.97	300.41	85.06%	144.00	43.10	391.82	257.52	14.28%
328.00	4.50	379.96	-125.18	400.04	94.98%	196.00	43.30	393.64	387.92	3.03%
372.00	6.00	359.38	-174.87	399.67	89.92%	190.00	40.41	367.36	407.20	1.88%
423.00	6.90	339.79	-210.71	399.82	84.99%	183.00	42.00	381.82	369.29	7.64%
432.00	3.10	477.03	-154.42	501.40	95.14%	226.00	42.70	388.18	472.20	5.82%
480.00	4.20	452.58	-216.97	501.90	90.17%	223.00	41.80	380.00	476.84	4.99%
535.00	5.00	423.56	-263.51	498.83	84.91%	215.00	41.10	373.64	465.43	6.70%
536.00	2.40	570.75	-186.20	600.35	95.07%	259.00	41.80	380.00	571.58	4.79%
589.00	3.30	539.03	-261.98	599.32	89.94%	253.00	40.80	370.91	572.11	4.54%
650.00	3.90	507.74	-316.76	598.44	84.84%	247.00	40.20	365.45	565.87	5.44%
641.00	2.00	661.54	-222.13	697.83	94.80%	291.00	41.00	372.73	670.73	3.88%
699.00	2.70	627.19	-306.65	698.14	89.84%	283.00	39.80	361.82	672.16	3.72%
765.00	3.20	590.69	-369.68	696.84	84.77%	277.00	39.00	354.55	671.28	3.67%
746.00	1.60	764.04	-245.25	802.43	95.21%	320.00	40.30	366.36	763.45	4.86%
809.00	2.20	726.32	-344.61	803.92	90.35%	312.00	39.10	355.45	767.75	4.50%
882.00	2.70	675.49	-423.06	797.04	84.75%	302.00	38.00	345.45	764.21	4.12%
851.00	1.40	856.43	-279.38	900.85	95.07%	346.00	39.40	358.18	855.99	4.98%
920.00	1.90	816.84	-388.16	904.38	90.32%	335.00	38.20	347.27	854.66	5.50%
998.00	2.30	766.57	-473.47	901.00	85.08%	325.00	37.30	339.09	848.45	5.83%

956.00	1.20	956.10	-304.94	1,003.55	95.27%	375.00	38.80	352.73	953.14	5.02%
1,031.00	1.70	901.14	-435.62	1,000.90	90.03%	360.00	37.40	340.00	948.82	5.20%
1,115.00	2.00	857.92	-523.97	1,005.27	85.34%	351.00	36.40	330.91	950.71	5.43%
1,061.00	1.10	1,045.27	-342.92	1,100.08	95.02%	400.00	38.10	346.36	1,044.86	5.02%
1,141.00	1.50	995.11	-475.91	1,103.06	90.21%	386.00	36.70	333.64	1,046.95	5.09%
1,232.00	1.80	936.42	-578.95	1,100.94	85.06%	373.00	35.60	323.64	1,042.53	5.31%
1,166.00	1.00	1,138.05	-376.59	1,198.74	94.94%	423.00	37.30	339.09	1,137.45	5.11%
1,252.00	1.40	1,070.69	-529.01	1,194.25	89.65%	404.00	35.90	326.36	1,127.88	5.56%
1,349.00	1.60	1,034.10	-626.62	1,209.14	85.52%	400.00	35.00	318.18	1,147.14	5.13%
,271.00	0.9	1,235.63	-404.51	1,300.16	95.04%	440.00	36.60	332.73	1,212.40	6.75%
1,363.00	1.20	1,188.30	-554.07	1,311.12	90.63%	429.00	35.20	320.00	1,230.63	6.14%
1,466.00	1.50	1,102.38	-685.57	1,298.17	84.92%	414.00	34.10	310.00	1,225.48	5.60%
1,377.00	0.8	1,339.72	-425.58	1,405.69	95.31%	463.00	35.90	326.36	1,308.66	6.90%
1,474.00	1.10	1,280.34	-596.14	1,412.32	90.65%	445.00	34.40	312.73	1,312.97	7.03%
1,584.00	1.40	1,176.41	-742.94	1,391.37	84.55%	427.00	33.30	302.73	1,300.51	6.53%

Even though the procedures above yielded satisfactory results and were in compliance with the guidelines presented in 2, one more trial was designed. Also mentioned in Chapter 2 (Figure 2.2), the complete human body equivalent circuit acquired by Chinen et al.[22] was also used as a test load. This circuit, when simplified, will generate a circuit similar to the ones used in the previous test, but nonetheless it was decided to use it to mitigate any differences between the equivalent circuit and the human body. Since the designed device would measure the bioimpedance using the "arm-to-arm" path, the capacitance and resistance values used can be seen in Figure 4.10 while the result from the measurement can be seen in Table 4.5.
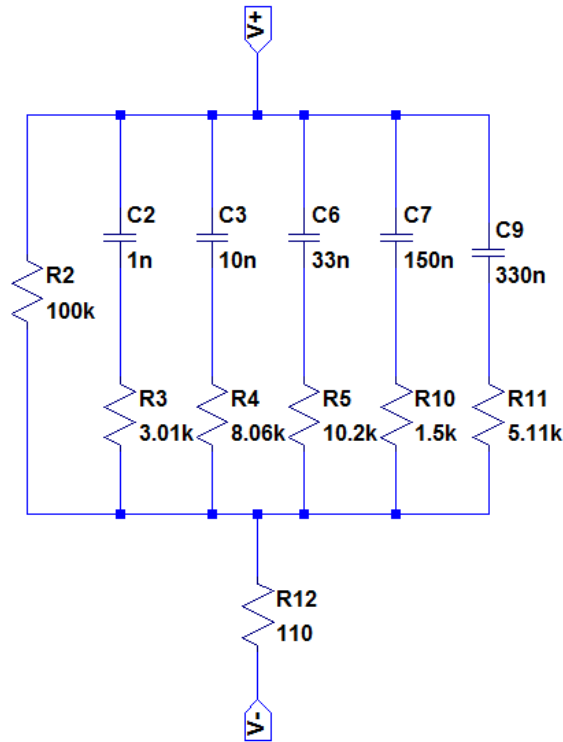

Figure 4.10: Equivalent circuit with 5 High Pass filters showing resistor and capacitor values used on the test.

Table 4.5: Results from trial with equivalent circuit in Figure 4.10.

$V_1(mV)$	$V_2(mV)$	$I(\mu A)$	$R_{measured}(\Omega)$	$Z_{nominal}(\Omega)$	Error
349.00	41.40	376.36	817.29	900.10	9.20%

Chapter 5

Conclusions

5.1   Results Discussion

This monograph proposed the implementation of a system that would generate recommendations regarding the safe practice of physical activities using contextual information about the user and the environment. As explained throughout the text, the first prototype of such system was developed and presented in [27] and [28]. These publications, though, focused on the development of the java application, using very crude methods to acquire the relevant data. An update to the application, made in 2014 included a pulse rate measurement system and the development of the custom-made weight scale. Although still rudimentary, these prototypes allowed the verification of the system, generating personalised recommendations to the user once the data was inserted. With that in mind, the main focus of this work was to further develop the data acquisition modules and to properly validate them. The acquisition modules were developed according to the procedures described in Chapter 3.

Chapter 4 dissects the experimental methodology used to validate the developed modules and presents the results from the performed trials. The pulse rate detector circuit was evaluated against the simulations and other commercially available systems and presented a steady performance. Even though the results were promising, few tests were carried out and the device was not compared to clinical equipment or with any established standards. That said, the system in question is not intended to be used in clinical environments nor does it intend to replace professional advice so the data acquired is a good indication that the circuit developed performs adequately for the intended purposes.

The BIA device was tested using electrical circuits equivalent to the human body and the circuit designed proved to be able to satisfactorily estimate the impedance for loads with 85%, 90%, 95% and 100% resistive characteristics. Also, it worked well for all equivalent circuit models. On the other hand, the current regulation, even though prevented the current from reaching dangerous levels, was very poor, having a large variation within the load range of interest, which could be cause for some of the inaccuracies in measurement. Despite of this downside, the variation was not enough to prevent the assessment of the impedance, so the results can be considered satisfactory

even if it has room for improvements.

5.2 Future Contributions

Unfortunately, it was not possible to alter the original system to replace the old data acquisition modules with the new ones, but since the system had been previously validated, and the modules were individually tested, it is expected that these modifications will be feasible. To achieve this goal, it is necessary to build a mechanically robust structure for the weight scale, replace the pulse rate detection routine, and add the bioimpedance computation routine. In addition to that, it is expected to replace the old user interface used in the customised recommendation for the new one, using the real time graphic representation of the PPG signal as shown in Figure 5.1.

Also, since the production rules responsible for the creation of a recommendation had already been built by the time the pulse rate monitor was designed, the system currently delivers two separate recommendations, one regarding the resting heart rate and one with respect to the remaining data. These production rules should be unified to provide better guidance to the user.

Moreover, the **BIA** device should be better tested and human trials might be considered as well as performing additional tests according to the necessary regulations to use it in clinical applications. Furthermore, the performance of this module can and should be improved.

In addition to that, a few studies such as Shin and Min's [32], Xing and Sun's [33] and Jeong, Ko and Hwang's [34], suggest that the PPG signal can be used as an non-invasive method for assessing blood pressure. With that taken into consideration, with the necessary modifications, a new measurement could be taken without the need for a new module, thus generating an even better recommendation.

A possible interface with a smartphone application has also been considered, as well as adjustments in the system for use during the practice of physical exercise.
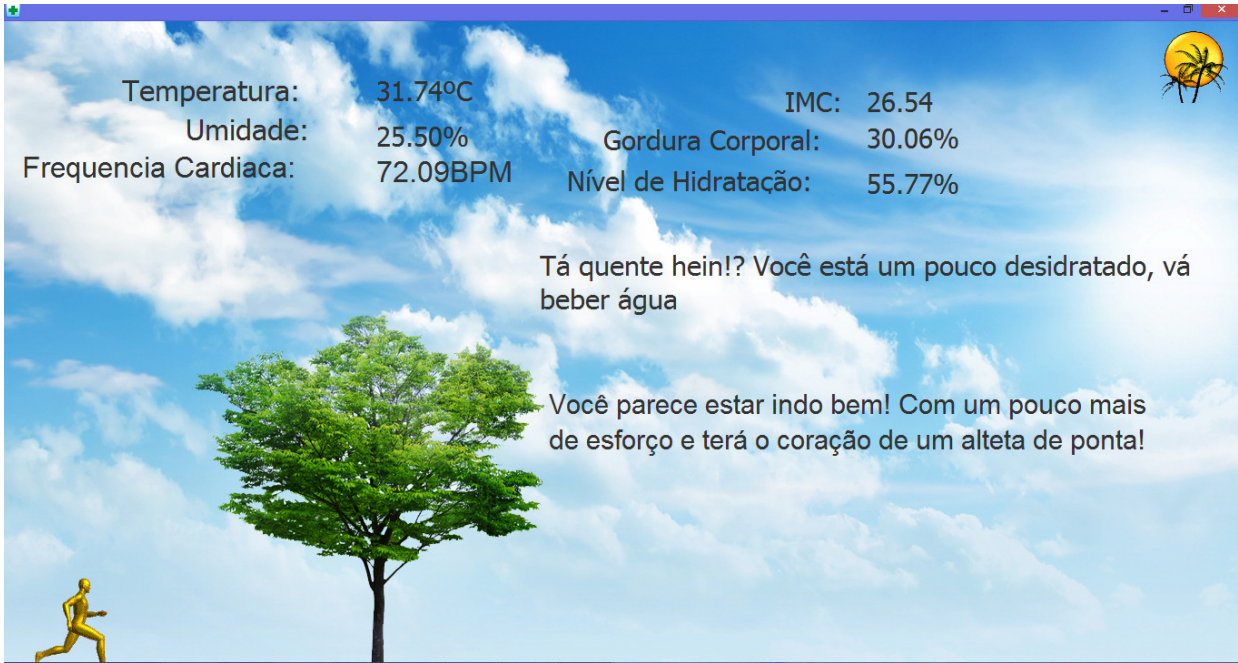
(a) Simulation of current system's graphic interface using randomly generated data
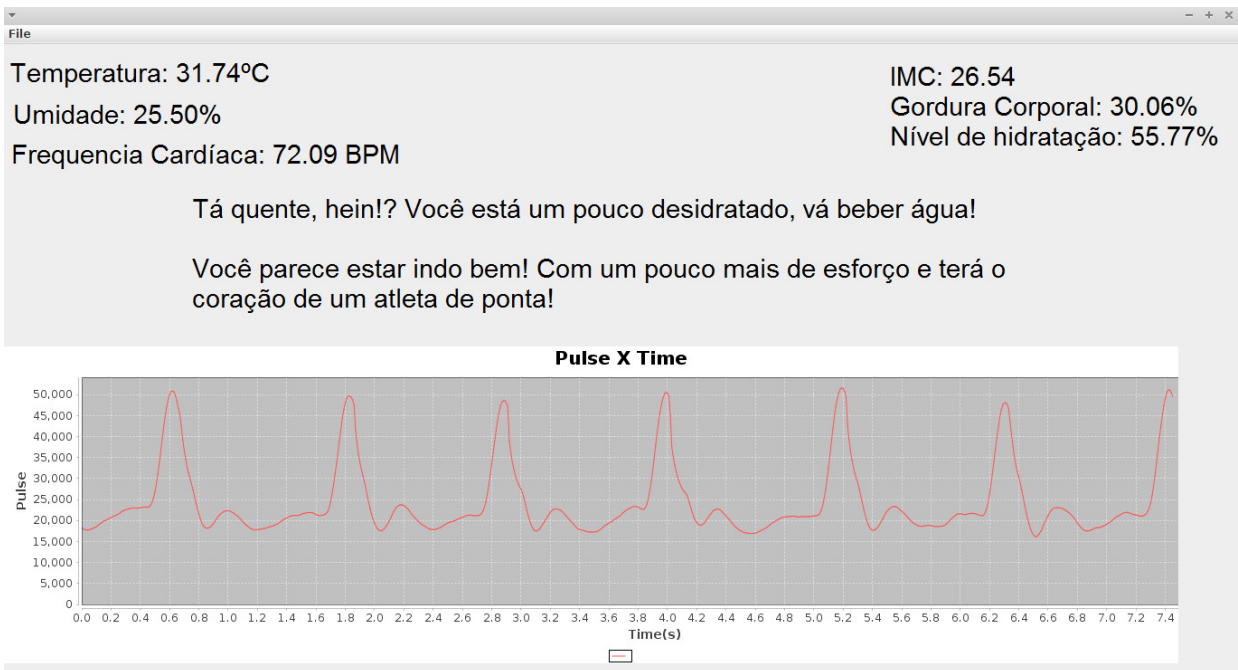
(b) Model of system's new graphic interface data from the simulation data from 5.1(a)

Figure 5.1: Comparison between current system's graphic interface and the suggested graphic interface developed for the new Pulse Rate Monitor Device

BIBLIOGRAPHIC REFERENCES

[1] ORGANIZATION, W. H. et al. *Global status report on noncommunicable diseases 2010.* [S.l.]: Geneva: World Health Organization, 2011.

[2] OBESITY and Overweight Fact Sheet. 2017. Disponível em: <http://www.who.int/mediacentre/factsheets/fs311/en/>.

[3] PHYSICAL Inactivity: A Global Public Health Problem. 2017. Disponível em: <http://www.who.int/dietphysicalactivity/factsheet_inactivity/en/>.

[4] MARINS, J. Exercício físico e calor: Implicações fisiológicas e procedimentos de hidratação. *Revista Brasileira de Atividade Física e Saúde*, v. 1, 1996.

[5] DEY, A. K. Understanding and using context. *Personal Ubiquitous Comput.*, Springer-Verlag, London, UK, UK, v. 5, n. 1, p. 4–7, jan. 2001. ISSN 1617-4909. Disponível em: <http://dx.doi.org/10.1007/s007790170019>.

[6] VENTURELLI, S.; BARRETTO, F. de P.; FREITAS, A. B. de. Biocyberurban parq: An ubiquitous and pervasive computing system for environmental integration. In: _____. *Universal Access in Human-Computer Interaction. Applications and Services for Quality of Life: 7th International Conference, UAHCI 2013, Held as Part of HCI International 2013, Las Vegas, NV, USA, July 21 − 26, 2013, Proceedings, Part III.* Berlin, Heidelberg: Springer Berlin Heidelberg, 2013. p. 116–124. ISBN 978-3-642-39194-1.

[7] SEELEY R; VANPUTTE, C. R. J. R. A. *Seeley's Anatomy & Physiology.* [S.l.]: Mcgraw-Hill, 2014.

[8] MCARDLE, W.; KATCH, F.; KATCH, V. *Exercise Physiology: Nutrition, Energy, and Human Performance.* [S.l.]: Lippincott Williams & Wilkins, 2010. (Point (Lippincott Williams & Wilkins)). ISBN 9780781797818.

[9] COUNCIL, N. et al. *Expanding the Vision of Sensor Materials.* National Academies Press, 1995. ISBN 9780309176750. Disponível em: <https://books.google.com.br/books?id=Ao5W46ag9XwC>.

[10] FARAHANI, H.; WAGIRAN, R.; HAMIDON, M. N. Humidity sensors principle, mechanism, and fabrication technologies: A comprehensive review. *Sensors*, v. 14, n. 5, p. 7881–7939, 2014. ISSN 1424-8220. Disponível em: <http://www.mdpi.com/1424-8220/14/5/7881>.

[11] ASSOCIATION, A. E. *Aquatic Fitness Professional Manual.* [S.l.]: Human Kinectics, 2010.

[12] COMMITTEE CENTRE FOR HEALTH PROTECTION, D. o. H. E. P. D. *Exercise Prescription Doctor's Handbook.* [s.n.], 2012. Disponível em: <http://exerciserx.cheu.gov.hk/files/DoctorsHanbook_fullversion.pdf>.

[13] ALLEN, J. Photoplethysmography and its application in clinical physiological measurement. *Physiological Measurement*, v. 28, 2007.

[14] NETWORK, S. I. G. *Management of Obesity: A National Guideline.* [S.l.: s.n.], 2010.

[15] WAN, C. S. et al. Bioelectrical impedance analysis to estimate body composition, and change in adiposity, in overweight and obese adolescents: comparison with dual-energy x-ray absorptiometry. *BMC Pediatrics*, v. 14, n. 1, p. 249, 2014. ISSN 1471-2431. Disponível em: <http://dx.doi.org/10.1186/1471-2431-14-249>.

[16] MUTH, N. D. *What are the guidelines for percentage of body fat loss?* 2017. Disponível em: <https://www.acefitness.org/acefit/healthy-living-article/60/112/what-are-the-guidelines-for-percentage-of-body-fat>.

[17] MCQUEEN, M. A. Exercise aspects of obesity treatment. *The Ochsner Journal*, v. 9, n. 3, 2009. Disponível em: <https://www.ncbi.nlm.nih.gov/pmc/articles/PMC3096271/>.

[18] LIPIANSKY, E. *Electrical, electronics, and digital hardware essentials for scientists and engineers.* 1. ed. [S.l.]: Wiley, 2013.

[19] BIOELECTRICAL Impedance Analysis in Body Composition Measurement: National Institutes of Health Technology Assessment Conference Statement. *The American Journal of Clinical Nutrition*, v. 64, p. 524 to 532, 1996.

[20] DEHGHAN, M. Is bioelectrical impedance accurate for use in large epidemiological studies? *Nutrition Journal*, v. 7, n. 26, 2008.

[21] AROOM KEVIN R.; HARTING, M. T. C. J. C. S. R. R. S. S. C. G. B. S. Bioimpedance analysis: A guide to simple design and implementation. *Journal of Surgical Research*, v. 153, 2009.

[22] CHINEN KOYU; KINJO ICHIKO; ZAMAMI, A. I. K. N. K. *New Equivalent Electrical Circuit Model and a Practical Measurement Method for Human Body Impedance.* [S.l.: s.n.], 2015.

[23] RAZAVI, B. *Design of Analog CMOS Integrated Circuits.* [S.l.]: Mcgraw-Hill, 2015.

[24] ALURU, G. *Exploring Analog and Digital Design Using the Open-Source Electric VLSI Design System.* Dissertação (Mestrado) — University of North Texas, 5 2016.

[25] RAO, B. *Electronic Circuit Analysis.* [S.l.]: Pearson, 2012. ISBN 9788131754283.

[26] SENANI, R. et al. *Sinusoidal Oscillators and Waveform Generators using Modern Electronic Circuit Building Blocks.* [S.l.]: Springer International Publishing, 2015. ISBN 9783319237121.

[27] BASTOS MATHEUS S; TIVERON BORGES, T. d. M. S. G. P. R. G. N. A. R. Aplicação para recomendação contextualizada sobre atividades físicas aos usuários do parque da cidade. In: *12º Encontro Internacional de Arte e Tecnologia - #12ART*. [S.l.: s.n.], 2013.

[28] BASTOS, M. S.; BORGES, T. d. M. T. *Aplicação para recomendação Contextualizada sobre atividades físicas aos usuários do Parque da Cidade*. Dissertação (Undergraduate Dissertation) — IESB - Instituto de Educação Superior de Brasília, 11 2013.

[29] Maxdetect. *Digital relative humidity and temperature sensor RHT03 datasheet*. Disponível em: <http://cdn.sparkfun.com/datasheets/Sensors/Weather/RHT03.pdf>.

[30] CLASS for DHTxx Sensors. 2017. Disponível em: <http://playground.arduino.cc/Main/DHTLib>.

[31] BHATT, R. *Introducing Easy Pulse: A DIY photoplethysmographic sensor for measuring heart rate - Embedded Lab*. 2012. Disponível em: <http://embedded-lab.com/blog/introducing-easy-pulse-a-diy-photoplethysmographic-sensor-for-measuring-heart-rate/>.

[32] SHIN, H.; MIN, S. D. Feasibility study for the non-invasive blood pressure estimation based on ppg morphology: normotensive subject study. *BioMedical Engineering OnLine*, v. 16, n. 1, 2017.

[33] XING, X.; SUN, M. Optical blood pressure estimation with photoplethysmography and fft-based neural networks. *Biomedical Optics Express*, v. 7, n. 8, p. 3007, 2016.

[34] JEONG, I. C. et al. A new method to estimate arterial blood pressure using photoplethysmographic signal. In: *2006 International Conference of the IEEE Engineering in Medicine and Biology Society*. [S.l.: s.n.], 2006. p. 4667–4670. ISSN 1557-170X.

[35] IRWIN J. DAVID; NELMS, R. M. *Basic Engineering Circuit Analysis*. [S.l.]: John Wiley & Sons, 2008.

[36] IRWIN J. DAVID; NELMS, R. M. *Basic Engineering Circuit Analysis*. [S.l.]: John Wiley & Sons, 1993.

[37] GLISSON, T. *Introduction to Circuit Analysis and Design*. [S.l.]: Springer Netherlands, 2011. ISBN 9789048194438.

APPENDIXES

I. BASIC ELECTRICAL ENGINEERING CONCEPTS

I.1 Introduction

As a multidisciplinary work, this monograph is aimed at an audience broader than that of the Electrical Engineering field, and as such, some of the concepts that may be considered basic to Electrical Engineers and Electrical Engineering students may not be so to readers from other fields related to Biomedical Engineering or Exercise Physiology. Being so, this Chapter provides a brief introduction the the core concepts that were explored in this text.

I.2 Operational Amplifiers

To implement a **BIA** module capable of measuring bioimpedance without harming the users, it was necessary to build a circuit that would limit the output current. This section is dedicated to explain the theory behind operational amplifiers and, ultimately, how to use them to build a current source.

Ideally, Operational Amplifiers can be modelled as a three-terminal component (two input terminals and one output terminal) with an infinite input impedance creating the equivalent of an open circuit, a zero output impedance, creating the equivalent of a short circuit, and a controlled voltage source with infinity gain, which demands for an infinitesimally small voltage between the two input terminals as explained by David Irwin in [35]. Following these ideal characteristics, the operational amplifier works by amplifying the difference between the two inputs, generating an amplified voltage in the output. The infinity gain, although desired in the operational amplifier, yields no practical use, since it would generate infinite voltages in the output, so in real applications, the amplifier gain can be limited by the network connected to it. The ideal circuit, as well as its representation can be seen in Figure I.1 adapted from [35].
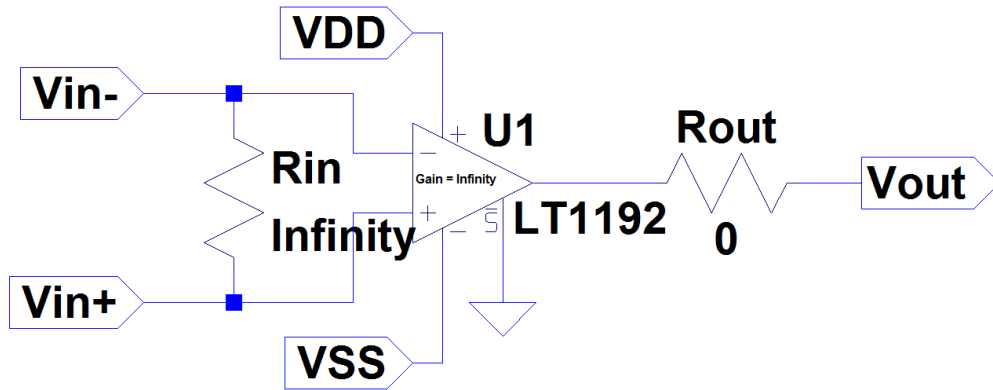
Figure I.1: Ideal Operational Amplifier Model.

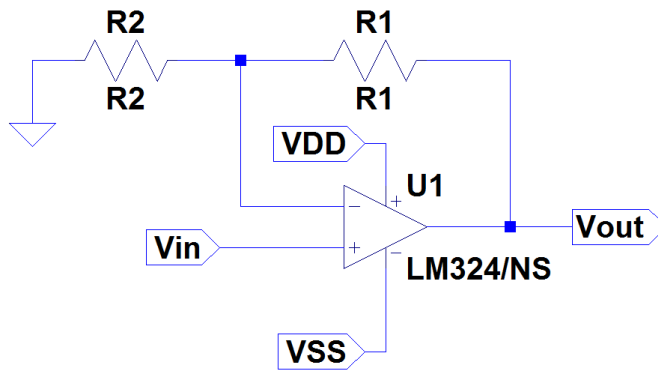### I.2.1 Common Configurations

The two inputs in an operational amplifier allows for a plethora of different uses. Three of the most common configurations are the Unity-Gain Buffer, the Inverting Amplifier and the Non-Inverting Amplifier (described in Figure I.2). These configurations rely on the fact that when a positive signal is connected to the positive input, the output will be positive as well, but if the same signal is connected to the negative input, the output will be negative.
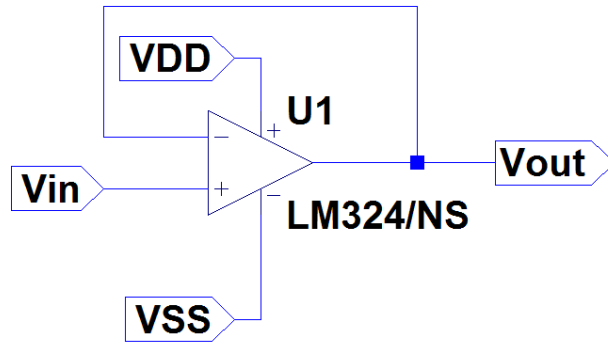
(a) Unity-Gain Buffer.
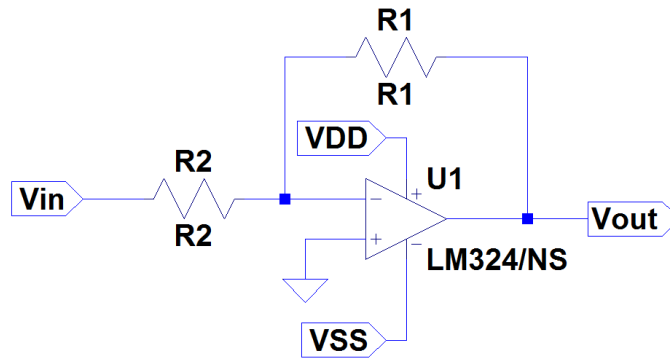
(b) Inverting Amplifier.

(c) Non-Inverting Amplifier.

Figure I.2: Common Amplifier Configurations.

The inverting amplifier, then, is a configuration in which the signal is connected to the negative input and the output is fed back into the same input using a resistive network. By using the ideal model of the operational amplifier, the circuit's gain, defined as the ratio of the signal voltage in the output to the signal voltage in the input, can be found to be given by I.1.

$$A_v = \frac{V_{out}}{V_{in}} = -\frac{R_2}{R_1} \tag{I.1}$$

The non-inverting amplifier, on the other hand, is the configuration in which the signal is connected to the positive input and the feedback network connects the output to the negative input and yields a gain given by I.2

$$A_v = \frac{V_{out}}{V_{in}} = 1 + \frac{R_2}{R_1} \tag{I.2}$$

It is interesting to note that the gain expression for the inverting amplifier allows it to work as an attenuator (gain smaller than unity), whereas the non-inverting amplifier always has a gain larger than one.

The Unity-gain buffer, as the name states, is a configuration where voltage gain is unity, and therefore the output is the same as the input. This configuration will not be further detailed here due to its simplicity, but can be found in any circuits textbook that covers operational amplifiers such as Irwin's[35] and [36].

I.3   Filters

Frequency selectivity in an electrical circuit is a property that causes some sinusoidal inputs to be more attenuated or amplified than others depending on their frequencies, as as described by Glisson in [37]. Filters are circuits designed to apply different gains to specific frequencies, thus allowing certain components of a signal to reach the load and preventing others from doing so. Filters can be classified according to the kind of elements used in them (passive or active) or their frequency bands (lowpass, bandpass, bandstop, highpass). Other classifications of filters are possible but will not be discussed in the scope of this work.

I.3.1   Frequency-Domain Analysis

Frequency-domain is a mathematical tool that allows the representation and analysis of sinusoidal signals as a functions of frequency instead of time. The ability to represent any electrical signal over a finite interval as a sum of sinusoids, as well as the superposition property of linear circuits, broadens the usefulness of this analysis to a much wider range of signals according to Glisson in [37]. In filters, the Frequency-Domain can be used to analyse these circuits according to the frequency bands they allow to pass (passbands) or block (stopbands). Filters that allow low frequencies to pass, but block high frequencies are called "lowpass filters", whereas filters that block only low frequencies but allows high frequencies to pass are called "highpass filters". Bandpass filters are filters that block everything higher or lower then a certain frequency that they allow to pass, whereas bandstop filters block a very specific band allowing all frequencies, higher or lower than the stopband, to pass. The measurement of the voltage transfer function of a circuit is often referred to as Frequency-Response Analysis.

I.3.2   Passive Filters

Passive filters are designed to contain solely passive components (e.g resistors, capacitors, inductors) and require no external power supply, but are often large and heavy. Also, this kind of filter does not provide gain, only attenuation, which sometimes limits its uses.

I.3.3   Active Filters

Active filters are designed using active components such as transistors or operational amplifiers. They often provide gain greater than unity to their passbands, while providing attenuation to their stopbands.This characteristic allows them to be connected as a cascade of filters, thus improving the gain in the passband and sharpening the cutoff.